

**DYNAMIC ANALYSIS OF HEATING, VENTILATING AND COOLING
MODULE PARTS OF AUTOMOBILE AIR CONDITIONING SYSTEM**

*A dissertation report submitted in partial fulfilment of the requirement for the
award of*

**MASTER OF ENGINEERING
IN
CAD/CAM & ROBOTICS**

Submitted By

PARDEEP KUMAR

Roll No. 801181021

Under the Guidance of

Mr. DALJEET SINGH

Assistant Professor

Mechanical Engineering Department,

Thapar University, Patiala



DEPARTMENT OF MECHANICAL ENGINEERING

THAPAR UNIVERSITY

PATIALA-147004, INDIA

July-2013

DECLARATION


I hereby declare that the work in this dissertation entitled "**DYNAMIC ANALYSIS OF HEATING, VENTILATING AND COOLING MODULE PARTS OF AUTOMOBILE AIR CONDITIONING SYSTEM**" is an authentic record of my study carried out as fulfilment for the award of degree of **Master of Engineering in CAD/CAM & Robotics** at **Thapar University, Patiala** under the guidance of **Mr. Daljeet Singh**, Assistant Professor, Mechanical Engineering Department, Thapar University, Patiala in **July 2013**.

The matter embodied in this report has not been submitted in part or full to any other university or institute for the award of any other degree.


(Pardeep Kumar)

Reg. No. 801181021

This is to certify that above declaration made by the student concerned is correct to the best of my knowledge and belief.

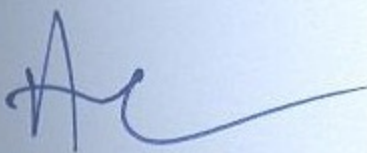

(Mr. DALJEET SINGH)

(Assistant Professor)

Mechanical Engineering Department

Thapar University, Patiala-147004

Countersigned by:


(Dr. AJAY BATISH)

Professor and Head,
Mechanical Engineering Department
Thapar University, Patiala-147004


(Dr. S.K. MOHAPATRA)

Dean of Academic Affairs,
Thapar University,
Patiala-147004

DECLARATION

I hereby declare that the work in this dissertation entitled “**DYNAMIC ANALYSIS OF HEATING, VENTILATING AND COOLING MODULE PARTS OF AUTOMOBILE AIR CONDITIONING SYSTEM**” is an authentic record of my study carried out as fulfilment for the award of degree of **Master of Engineering in CAD/CAM & Robotics** at **Thapar University, Patiala** under the guidance of **Mr. Daljeet Singh**, Assistant Professor, Mechanical Engineering Department, Thapar University, Patiala in **July 2013**.

The matter embodied in this report has not been submitted in part or full to any other university or institute for the award of any other degree.

(Pardeep Kumar)

Reg. No. 801181021

This is to certify that above declaration made by the student concerned is correct to the best of my knowledge and belief.

(Mr. DALJEET SINGH)

(Assistant Professor)

Mechanical Engineering Department

Thapar University, Patiala-147004

Countersigned by:

(Dr. AJAY BATISH)

Professor and Head,

Mechanical Engineering Department

Thapar University, Patiala-147004

(Dr. S.K. MOHAPATRA)

Dean of Academic Affairs,

Thapar University,

Patiala-147004

ACKNOWLEDGEMENT

*I am highly grateful to the authorities of Thapar University, Patiala for providing this opportunity to carry out the dissertation work. I would like to express a deep sense of gratitude and thank profusely my guide **Mr. Daljeet Singh** for his sincere and invaluable guidance, suggestions and attitude, which inspired me to submit this report in the present form. His dynamism and diligent enthusiasm have been highly instrumental in keeping my spirits high. His flawless and forthright suggestions blended with an innate intelligent application have crowned my task with success.*

I am deeply indebted to my parents for their inspiration and ever encouraging moral support, which enabled me to pursue my studies.

I am also very thankful to the entire faculty and staff members of Mechanical Engineering Department for their intellectual support and cooperation.

(Pardeep Kumar)

Reg. No.: 801181021

ABSTRACT

The automotive air-conditioning industry aiming at higher levels of quality, cost effectiveness and a short time to market, the need for simulation is at an all-time high. In the present work, the use of multibody dynamics approach is proposed in the simulation and analysis of the airflow control mechanisms of an automotive HVAC module for opening various doors/dampers used for passenger comfort. The movements of various parts have been kinematically and dynamically analysed. Two HVAC kinematic mechanism are analysed, one with single link configuration and other with two link configuration. Torque required in the two link configuration is lesser than in the single link configuration, thus lowering the effort required to rotate the cam from the control panel. Analyses are also done by varying the speed of cam, and by considering the friction between cam slots and pin, and air pressure on damper face. Flexible body analyses are also done and the stress is obtained at different speeds.

INDEX

Title	Page No.
Declaration	i
Acknowledgement	ii
Abstract	iii
Index	iv
List of figures	vi
List of tables	ix
Nomenclature and abbreviations	x
CHAPTER-1: INTRODUCTION	1-11
1.1 Computer Aided Engineering	1
1.1.1 Advantages of CAE	2
1.1.2 Disadvantages of CAE	2
1.2 Simulation (Analysis) steps for generic CAE software	2
1.2.1 CAE Commercial software	3
1.2.2 Analysis process for CAE	4
1.3 Multibody Systems	5
1.3.1 Degree of freedom	5
1.3.2 Dependent and Independent Coordinates	6
1.3.3 Kinematic and Dynamic Analysis of Multibody Systems	8
1.3.4 Equation of Motion	9
1.3.5 Dynamic Analysis Process	9
CHAPTER-2: LITERATURE REVIEW	12-21
2.1 Literature Review	12
CHAPTER 3: HVAC KINEMATIC MECHANISM SIMULATION	22-33
3.1 Problem Definition	22
3.2 Introduction to HVAC Kinematic Mechanism	23
3.3 Design and Analysis Cycle of HVAC	24

3.4 Kinematic Analysis of HVAC Mechanism	24
3.4.1 Reverse Engineering of HVAC Components	25
3.4.2 CAD Modelling of HVAC Components	26
3.4.3 Mass and Inertia Properties of HVAC Components	26
3.4.4 Discretization of CAD Geometry	27
3.4.5 Pre- Processing	28
3.4.6 Solution	32
3.4.7 Post Processing	32
CHAPTER 4: EFFECT OF VARIATION IN SPEED	34-40
4.1 Introduction	34
4.1 Pre-Processing	35
4.1 Results	35
CHAPTER 5: SIMULATION WITH FRICTION	41-45
5.1 Introduction	41
5.2 Results	42
CHAPTER 6: EFFECT OF FORCE DUE TO AIR PRESSURE ON DAMPER	46-48
6.1 Introduction	46
6.2 Results	46
CHAPTER 7: FLEXIBLE BODY SIMULATION	49-57
7.1 Introduction	49
7.2 Results	50
7.3 Force on Link Analysis	52
7.4 Static Stress Analysis	54
CHAPTER-8: CONCLUSION AND SCOPE FOR FUTURE WORK	58-59
8.1 Conclusion	58
8.2 Scope for Future Work	59
REFERENCES	60-61

LIST OF FIGURES

Figure No.	Title	Page No.
1.1	Analysis process for CAE	4
1.2	Degrees of freedom of a rigid body in space	6
1.3	Four bar mechanism	7
1.4	Overview of the dynamic analysis	10
2.1	Components of car AC system	13
2.2	HVAC kinematic mechanism	14
3.1	Components of car AC system	22
3.2	HVAC kinematic mechanism	23
3.3	Slot 1 Profile	25
3.4	Slot 2 Profile	26
3.5	Exploded view of Assembly	26
3.6	Fine meshing done to pins and cam slots	27
3.7	Normal vectors of contact surfaces face each other	27
3.8	Points and bodies created	29
3.9	Joints created	29
3.10	Graphics for contact	30
3.11	Cam vs. Foot damper rotation	32
3.12	Cam vs. Face damper rotation	33
3.13	Cam rotations vs. Torque on cam	33
4.1	Single link mechanism	34
4.2	Double link mechanism	34
4.3	Cam rotation vs. Torque on cam at speed 1°/sec	35
4.4	Cam rotation vs. Torque on cam at speed 5°/sec	35
4.5	Cam rotation vs. Torque on cam at speed 10°/sec	36
4.6	Cam rotation vs. Torque on cam at speed 20°/sec	36
4.7	Cam rotation vs. Torque on cam at speed 30°/sec	36
4.8	Cam rotation vs. Torque on cam at speed 40°/sec	37

4.9	Cam rotation vs. Torque on cam at speed 50°/sec	37
4.10	Cam rotation vs. Torque on cam at speed 60°/sec	37
4.11	Cam rotation vs. Torque on cam at speed 80°/sec	38
4.12	Cam rotation vs. Torque on cam at speed 100°/sec	38
4.13	Cam rotation vs. Torque on cam at speed 1°/sec	38
4.14	Cam rotation vs. Torque on cam at speed 5°/sec	39
4.15	Cam rotation vs. Torque on cam at speed 10°/sec	39
4.16	Cam rotation vs. Torque on cam at speed 50°/sec	39
4.17	Cam rotation vs. Torque on cam at speed 60°/sec	40
4.18	Cam rotation vs. Torque on cam at speed 70°/sec	40
4.19	Cam rotation vs. Torque on cam at speed 80°/sec	40
5.1	Slot and Pin Graphics	41
5.2	Coefficient of friction	42
5.3	Cam rotation vs. Torque on cam at S=0.25, D=0.1	42
5.4	Figure 5.4: Cam rotation vs. Torque on cam at S=0.3, D=0.15	42
5.5	Figure 5.5: Cam rotation vs. Torque on cam at S=0.4, D=0.1	43
5.6	Cam rotation vs. Torque on cam at s=0.3, D=0.1	43
5.7	Cam rotation vs. Torque on cam at S=0.35, D=0.1	43
5.8	Cam rotation vs. Torque on cam at S=0.25, D=0.1	44
5.9	Cam rotation vs. Torque on cam at S=0.3, D=0.15	44
5.10	Cam rotation vs. Torque on cam at S=0.4, D=0.1	44
5.11	Cam rotation vs. Torque on cam at s=0.3, D=0.1	45
5.12	Cam rotation vs. Torque on cam at S=0.35, D=0.1	45
6.1	Cam rotation vs. Torque on cam at f=0.5N	46
6.2	Cam rotation vs. Torque on cam at f=1N	47
6.3	Cam rotation vs. Torque on cam at f=5N	47
6.4	Cam rotation vs. Torque on cam at f=10N	47
6.5	Cam rotation vs. Torque on cam at f=1.25N	48
6.6	Cam rotation vs. Torque on cam at f=10N	48
6.7	Cam rotation vs. Torque on cam at f=20N	48

7.1	Link with mesh	50
7.2	Nodal displacement of link	51
7.3	Cam rotation vs. Torque on Link at speed 10°/sec	52
7.4	Cam rotation vs. Torque on Link at speed 20°/sec	52
7.5	Cam rotation vs. Torque on Link at speed 40°/sec	53
7.6	Cam rotation vs. Torque on Link at speed 60°/sec	53
7.7	Cam rotation vs. Torque on Link at speed 80°/sec	53
7.8	Cam rotation vs. Torque on Link at speed 100°/sec	54
7.9	Stress analysis at speed of cam 10°/sec	54
7.10	Stress analysis at speed of cam 20°/sec	55
7.11	Stress analysis at speed of cam 40°/sec	55
7.12	Stress analysis at speed of cam 60°/sec	56
7.13	Stress analysis at speed of cam 80°/sec	56
7.14	Stress analysis at speed of cam 100°/sec	57

LIST OF TABLE

Figure No.	Title	Page No.
3.1	Coordinate data	28
3.2	Mass and inertia properties	29
7.1	Force analysis	54

NOMENCLATURE AND ABBREVIATIONS

HVAC	Heating, Ventilating and Cooling
MBS	Multibody system
AC	Air Conditioning
CAE	Computer Aided Engineering
CAD	Computer Aided Design
FEM	Finite Element Method
FVM	Finite Volume Method
FDM	Finite Difference Method
FEA	Finite Element Analysis
CFD	Computational Fluid Dynamics
COM	Centre of Mass
DAE	Differential Algebraic Equations
IGES	Initial Graphics Exchange Specification
DOF	Degrees of Freedom
HCF	Hybrid Coordinate Formulation

CHAPTER 1

INTRODUCTION

This introduction chapter discusses the basic details and concepts of related topics associated with the present work.

1.1 COMPUTER AIDED ENGINEERING (CAE)

There are many practical engineering problems for which we cannot obtain exact solutions. This inability to achieve an exact solution may be attributed to either the complex nature of governing differential equations or the difficulties that arise from dealing with the boundary and initial conditions. To deal with such problems, we help to numerical approximations. Compare with analytical solutions; show the exact behaviour of a system at any point inside the system, numerical solutions of approximate exact solutions only at discrete points.

For simple geometries, it is easy to visualize the point of the maximum stress and displacement. But in real life, parts or assemblies with complex geometrical shapes are made up of different materials with many discontinuities subjected to flexible constraints and complex loading varying with respect to time and point of application. This is further complex by residual stresses and joints like spot and arc welds etc. Because of this, it is not easy to predict the failure location. But with the help of CAD and CAE tools, if modelled in an appropriate fashion, anyone can easily get stress contour plots that clearly indicate the locations of high stress or displacement. CAD and CAE tools have made design and analysis faster and cheaper, reducing time to market, and making it possible to produce parts at lesser cost in the highly competitive automobile industry.

The use of computers is to help with all phases of engineering design work. Computer aided design(CAD) also involving the construction and analysis of objects, the idea is to use computer processing and interactive computer graphics to enable engineers to create, modify and analyse designs and hence to determine the structural, thermal, flow-field characteristics or other state of a system. CAE programs may use a geometry description from a CAD program as a starting point, and commonly utilize some form of finite element analysis (FEA) as the means to perform the analysis.

CAE used in analysis, simulation, design, manufacture and diagnosis. It encompasses simulation, validation and optimization of products and manufacturing tools.

Among the CAE areas covered include:

- Stress analysis on parts and assemblies using FEA.
- Computational fluid dynamics (CFD).
- Kinematics
- Mechanical event simulation (MES).
- Analysis tools used for process simulation for operations such as casting, moulding and die press forming.
- Optimization of the product.

1.1.1 Advantages of CAE

- Able to carrying out different engineering analyses such as, stresses and deformations, buckling, contact analyses, plastic deformations, vibration, heat transfer, fluid flow, coupled field problems, design optimization, etc.
- Can work shared with CAD systems.
- Analyses are simplified through GUI (Graphical User Interface).
- Material properties of different types can be included, isotropic, orthotropic, non-linear, etc.
- Reduction of time.
- Analysis and Simulation can be modified and updated easily.
- Graphical presentation of results.

1.1.2 Disadvantages of CAE

- High cost of CAE software.
- Required advanced and special hardware.
- Optical fatigue.
- Users training and qualification cost are high.

1.2 SIMULATION (ANALYSIS) STEPS FOR GENERIC CAE SOFTWARE

1. Modelling (Creation of Geometry)

The geometry is modelled using CAE package or geometry can be created and imported from separate CAD package.

2. Meshing of geometry (Discretization)

The entire domain of concern is subdivided to sub-domain to generate the desired mesh.

3. Defining material properties

This may include defining: Young's modulus, Poisson's ratio, shear modulus for structural analysis, heat capacity and thermal conductivity for thermal analysis, viscosity and density for fluid-flow analysis. Material could be solid, fluid, gas, liquid or composite.

4. Defining load

The term load includes all **boundary conditions** applied on system, however for transient analysis where variation with time occurred initial condition is required to define the state of system at time=0

5. Solution

At this stage, certain parameters is defined prior to run, this may include relaxation factors, accuracy, number of iteration, solver type.

6. Postprocessing

Postprocessing is used to review the analysis results over the entire model, or selected portion of the model for a specifically defined boundary conditions and/or initial conditions. This may include simple X-Y plot, 2-D & 3-D contour plot, carpet plot, vector plot, tabular data listing path plot, particle tracking, and complex data manipulation.

1.2.1 CAE Commercial Software

CAE software is used on various types of computers such as mainframes and superminis, grid-based computers, engineering workstations and personal computers. The choice of a computer system is based on the computing power required for the CAE application or the desired level and speed of graphics interaction. The different software used is:

- ANSYS
- Pro/Mechanica
- Nastran
- Hyper Mesh
- COSMOS Works
- LS-DYNA, LSTC

1.2.2 Analysis Process for CAE

Analysis process in CAE software can be divided into a series of stages as shown in fig (1.1). Taking each of the stages in sequence, it can be seen that the 1st stage requires no computing, the 2nd and 3rd stages require input from the analyst, the 4th stage involves computing but no actual input from the analyst and the 5th stage requires the analyst to evaluate the results.

An applicable set of CAE software might consist of three distinct phases:

1. Pre-processor phase
2. Solution phase
3. Post-processor phase

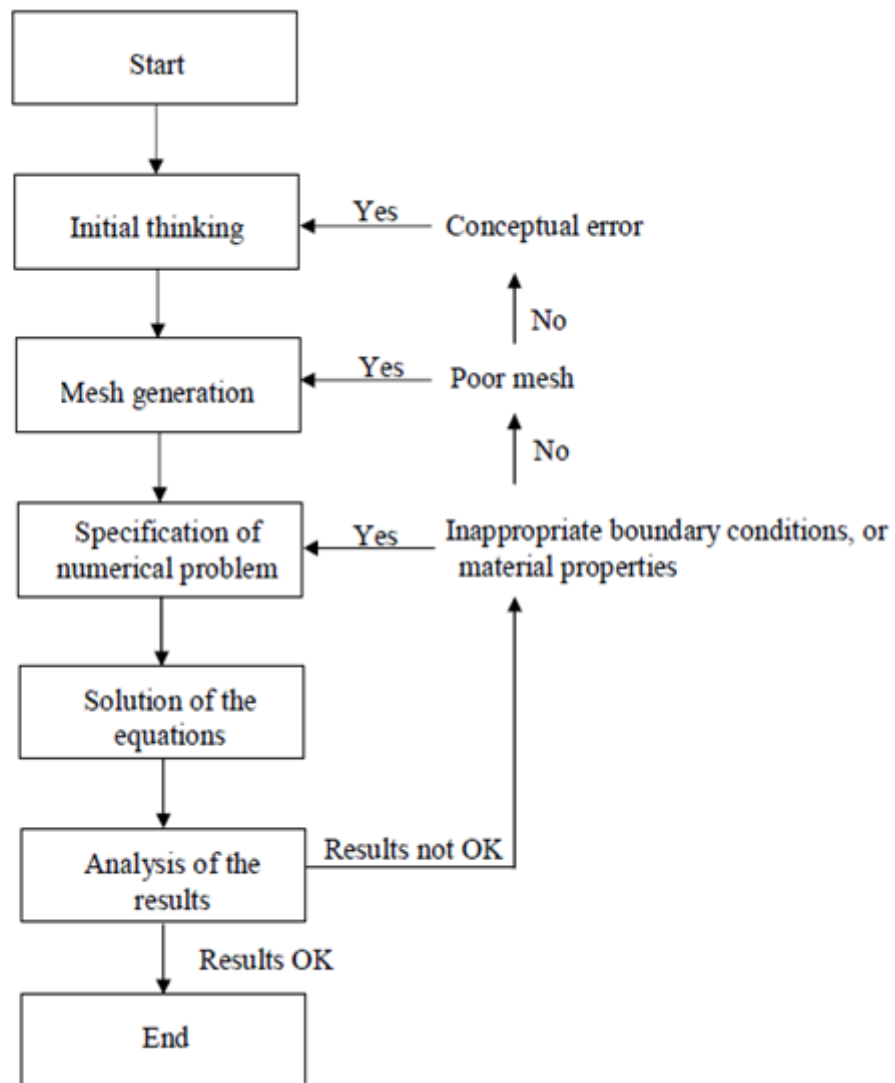


Figure 1.1: Analysis process for CAE

1.3 MULTIBODY SYSTEMS

A multibody system is generally defined as an assembly of bodies which interact with each other through joints that limit the motion possibilities of the interconnected bodies relative to each other.

Multibody systems are classified as open-chain or closed-chain systems. If a system is composed of bodies without closed branches or loops, then it is called an open chain system; otherwise, it is called a closed-chain multibody system. A double pendulum and a tree-type of system are good examples of an open-chain configuration. The four-bar mechanism is an example of a closed-chain system.

The joining of the two bodies that makes up a multibody system is called a kinematic pair or joint. A joint permits certain degrees of freedom of relative motion and prevents or restricts others.

Types of kinematic constraints include various types of joints e.g.:

- a) Revolute joints
- b) Translational joints
- c) Spherical joints
- d) Cylindrical joints

The slider-crank mechanism is a typical example of multibody system. The mechanism is used to transform rotational motion into translational motion by means of a rotating driving beam, a connection rod and a sliding body. Connection rod is used as a flexible body. The sliding mass is not allowed to rotate and three revolute joints are used to link the bodies. While each body has six degrees of freedom in space and the kinematical conditions lead to one degree of freedom for the whole system.

1.3.1 Degree of Freedom

Degrees of freedom are the minimum number of parameters required to completely define the position of an entity in space. It denotes the number of independent kinematical possibilities to move. An unrestrained rigid body in space has six degrees of freedom as shown in fig.1.2: three translating motions along the x , y and z axis and three rotary motions around the x , y and z axis respectively. A coordinate is one of these parameters.

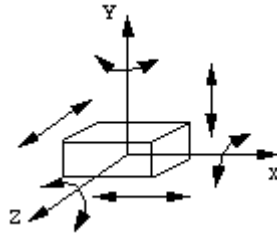


Figure 1.2: Degrees of freedom of a rigid body in space

1.3.2 Dependent and Independent Coordinates

To define a multibody system, the first essential point to consider is that of choosing a mathematical way or model that will describe its position and motion. In other words, select a set of parameters or coordinates that will permit one to unequivocally define the velocity, position and acceleration of the multibody system at all times.

There are two systems of coordinates:

- a) Independent coordinate system
- b) Dependent coordinate system

Independent coordinates system the number of coordinates coincides with the number of degrees of freedom of motion of the multibody system and is thereby minimal.

Dependent coordinates system, the number of coordinates larger than that of the degrees of freedom, which can describe the multibody system much more easily but which are not independent, but interconnected through certain equations known as constraint equations. The no. of constraints is equal to the variance between the number of dependent coordinates and the number of degrees of freedom. Constraint equations are generally nonlinear and play a main part in the kinematics and dynamics of multibody systems.

Independent coordinates are not a suitable solution for a general purpose analysis, because they do not meet one of the most important requirements: that the coordinate system should unequivocally define the position of the multibody system. Independent coordinates directly determine the position of the input bodies or the value of the externally driven coordinates, but not the position of the whole system. For some specific applications, independent coordinates can be useful to define with a minimum data set the actual velocities or accelerations and small variations in the position. In addition, they may lead to the maximum computational efficiency.

Fig. 1.3 shows a four-bar mechanism modeled with Cartesian coordinates of points 1 and 2. There are four dependent coordinates (x_1, y_1, x_2, y_2) and the mechanism has one degree of freedom. Hence, there should be three constraint equations relating the four dependent coordinates.

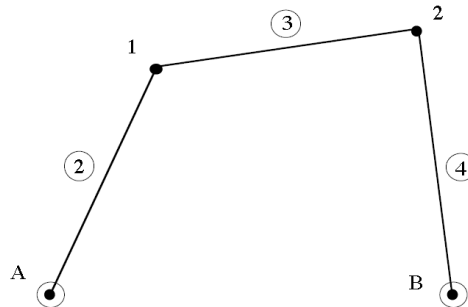


Figure 1.3: Four bar mechanism

The constraint equations shall guarantee that points 1 and 2 move in accordance with the limitations imposed on them by the three moving bars of the four-bar mechanism. It is precisely from there that the three constraint equations arise: from the fact of imposing the rigid body condition (a constant distance between points) on the three elements of the mechanism. These conditions can be formulated mathematically as follows:

$$(x_1 - x_A)^2 + (y_1 - y_A)^2 - l_2^2 = 0$$

$$(x_2 - x_1)^2 + (y_2 - y_1)^2 - l_3^2 = 0$$

$$(x_2 - x_B)^2 + (y_2 - y_B)^2 - l_4^2 = 0$$

These are the three constraint nonlinear equations that correspond to the mechanism shown. A similar system of equations can be established for any other type of coordinates and for any other multibody system.

Two types of Dependent coordinate systems which can be used are:

- a) Absolute dependent coordinate system - absolute coordinates define the position of each element in relation to a fixed reference frame.
- b) Relative dependent coordinate system - relative coordinates define the position of each link in relation to the previous link in the kinematic chain by using a parameter which corresponds to the relative degree of freedom allowed by the joint connecting the links.

1.3.3 Kinematic and Dynamic Analysis of Multibody Systems

In dealing with the study of multibody system motion, two different types of analysis can be performed:

- Kinematic analysis
- Dynamic analysis.

The kinematic analysis consists in the study of the system's motion independently of the forces that produce it. In particular, the kinematic analysis involves the determination of position, velocity and acceleration of the system components. In kinematic analysis, only the interaction between the geometry and the motions of the system is analysed and obtained. Since the interaction between the forces and the system's motion is not considered, the motion of the system need to be specified to some extent, that is, the kinematic characteristics of some driving elements need to be prescribed, while the kinematic motion characteristics of the remaining elements are obtained using the kinematic constraint equations, which describe the topology of the system.

In the kinematic analysis forces are not considered, the system motion is specified by driving elements that manage the system motion throughout the analysis, whereas the position, velocity and acceleration of the remaining elements are defined by kinematic constraint equations that describe the system topology. In the kinematic analysis, the number of driver constraints must be equal to the number of degrees of freedom of the multibody mechanical system. In short, the kinematic analysis is executed by solving a set of equations that result from the kinematic and driver constraints.

The dynamic analysis of multibody systems aims to understanding the relationship between the motion of the system parts and the causes that produce the motion including external applied forces and moments. The motion of the system is, in general, not prescribed, being its calculation one of the principal objectives of the analysis. The dynamic analysis also provides a way to estimate external forces that depend on the relative position between the system's components, such as the forces exerted by springs, dampers and actuators. Furthermore, it also possible to estimate the external forces that are developed as a consequence of the interaction between the system components and the surrounding environment, such as contact-impact forces and friction forces. The internal reaction forces and moments generated at the kinematic joints are also provided by the dynamic analysis. These reaction forces and moments prevent the occurrence of

the relative motions in the prescribed directions between the bodies connected via kinematic joints.

1.3.4 Equation of Motion

The equation, which defines the equilibrium condition of the system at each point in time, is represented as

$$m\ddot{u}(t) + b\dot{u}(t) + ku(t) = p(t)$$

The equation of motion accounts for the forces acting on the structure at each instant in time. Typically, these forces are separated into internal forces and external forces. Internal forces are found on the left-hand side of the equation, and external forces are specified on the right-hand side. The resulting equation is a second-order linear differential equation representing the motion of the system as a function of displacement and higher-order derivatives of the displacement.

The solution of the equation of motion for quantities such as displacements, velocities, accelerations, and/or stresses all as a function of time is the objective of a dynamic analysis. The primary task for the dynamic analyst is to determine the type of analysis to be performed. The nature of the dynamic analysis in many cases governs the choice of the appropriate mathematical approach. The extent of the information required from a dynamic analysis also dictates the necessary solution approach and steps.

1.3.5 Dynamic Analysis Process

Before conducting a dynamic analysis, it is important to define the goal of the analysis prior to the formulation of the finite element model. Consider the dynamic analysis process to be represented by the steps in Fig. 1.4. The analyst must evaluate the finite element model in terms of the type of dynamic loading to be applied to the structure. This dynamic load is known as the dynamic environment. The dynamic environment governs the solution approach (*i.e.*, normal modes, transient response, frequency response, etc.). This environment also indicates the dominant behaviour that must be included in the analysis (*i.e.*, contact, large displacements, etc.). Proper assessment of the dynamic environment leads to the creation of a more refined finite element model and more meaningful results.

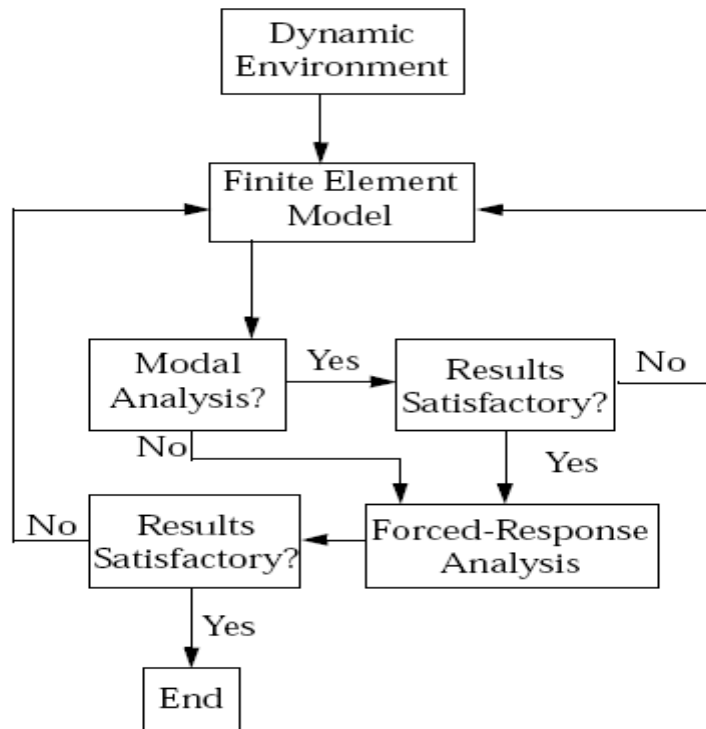


Figure 1.4: Overview of the dynamic analysis

An overall system design is formulated by considering the dynamic environment. As part of the evaluation process, a finite element model is created. This model should take into account the characteristics of the system design and, just as importantly, the nature of the dynamic loading (type and frequency) and any interacting media (fluids, adjacent structures, etc.). At this point, the first step in many dynamic analyses is a modal analysis to determine the structure's natural frequencies and mode shapes.

In many cases the natural frequencies and mode shapes of a structure provide enough information to make design decisions. For example, in designing the supporting structure for a rotating fan, the design requirements may require that the natural frequency of the supporting structure have a natural frequency either less than 85% or greater than 110% of the operating speed of the fan. Specific knowledge of quantities such as displacements and stresses are not required to evaluate the design.

Forced response is the next step in the dynamic evaluation process. The solution process reflects the nature of the applied dynamic loading. A structure can be subjected to a number of different dynamic loads with each dictating a particular solution approach. The results of a forced-response analysis are evaluated in terms of the system design. Necessary modifications are made to the system design. These changes are then applied

to the model and analysis parameters to perform iteration on the design. The process is repeated until an acceptable design is determined, which completes the design process.

The primary steps in performing a dynamic analysis are summarized as follows:

1. Define the dynamic environment (loading).
2. Formulate the proper finite element model.
3. Select and apply the appropriate analysis approach to determine the behaviour of the structure.
4. Evaluate the results.

The following section presents the review of the work done in kinematic and dynamic analysis of Multibody Systems.

2.1 LITERATURE REVIEW

A. Srivastava *et al.* [1] performed Multi-Body simulation of Earthmoving Equipment using Motion View / Motion Solve.

A. Srivastava *et al.* focuses on the problem description, solution and result correlation of a Hydraulic Excavator. The full cycle of operation consists of three major phases, Swing, Digging and Dumping. By defining the component under study as a flexible body, it is possible to retrieve stress values at gauge positions that are used in actual testing, which can be used to calculate fatigue life of welds. The input data available was 3D geometry of attachment, upper frame, lower frame and cabin, FE model of boom, Pressure on cylinder side and piston side of all cylinders during the cycle of operation, Stroke of all cylinders during the cycle of operation, Swing motor rotational speed during the cycle of operation. Output received was the reaction forces at each joints, severe position based on stress levels at specified strain gauge locations, Trace path of bucket tooth tip. It was concluded that CAE simulation can be used for kinematic design; thereby considerably reducing the Prototype costs.

B. He *et al.* [2] carried out failure analysis of an automobile damper spring tower.

A passenger car's damper spring tower early failures were investigated in this work. Inspection of the road surface, tire pressure, suspension and service load were firstly done. The static stress of the spring tower caused by the body weight was calculated by finite element model. The purpose of durability analysis was to reduce the development time and costs, prevent field failure, and optimize the vehicle structure. Component fatigue life is determined mainly by the load, material, design and manufacturing. Wheel force transducer (WFT) was used to measure the external load of the vehicle. Strain gauge, force transducer, and accelerometer were used for measuring the component local load. With the load spectrum, material properties and geometry model, multibody dynamics, finite element method, Manson Coffin equation was used for the simulation

and prediction of the fatigue life. It was concluded that the direct cause of the spring tower failure is the broken spring damper. From the comparison between tests, the spring damper's failure was partially caused by the elevated inflate pressure, bad road surface and more passengers (heavy load), because these factors increase the displacement of the spring damper and the collision frequency of the additional elastomer spring. Once the additional elastomer spring is broken, the spring damper will have no over compression protection and this will cause the piston's failure and leakage, so the failure of the spring damper will occur.

B. Singh *et al.* [3] carried out the kinematic analysis of heating, ventilating and cooling module parts of automobile air conditioning system using CAE tools.

An automotive air-conditioning system has an HVAC (as shown in Fig.2.1) module mounted on the firewall of the vehicle.

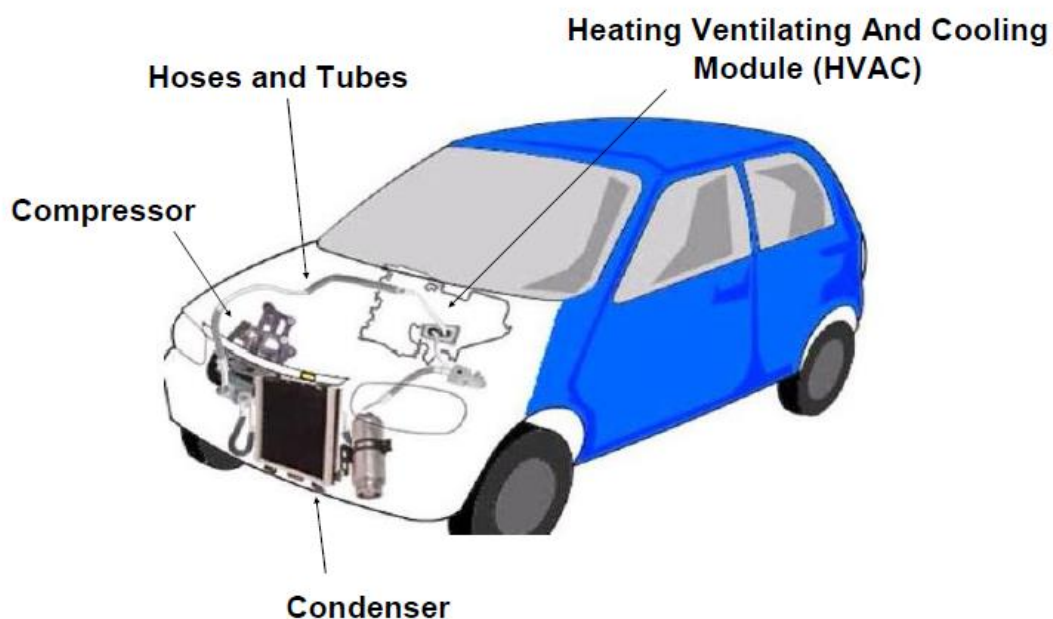


Figure 2.1: Components of car AC system

The use of multibody dynamics approach was proposed in the design and analysis of the airflow control mechanisms of an automotive HVAC module for opening various doors/dampers used for passenger comfort. The movements of various parts have been kinematically analysed. A new method for cam design was developed which was faster and simpler than the existing method. Two HVAC kinematic mechanism were designed, one with single link configuration and other with two link configuration for the same output. The assumptions include a constant angular velocity of the cam, and the rigidity

of the parts in the mechanism. Using the same simulation methodology, kinematic analysis was done for the two models and their results were compared.

The HVAC module parts considered for the analysis were: Cam, Links, Foot damper, Face damper (as shown in Fig.2.2).

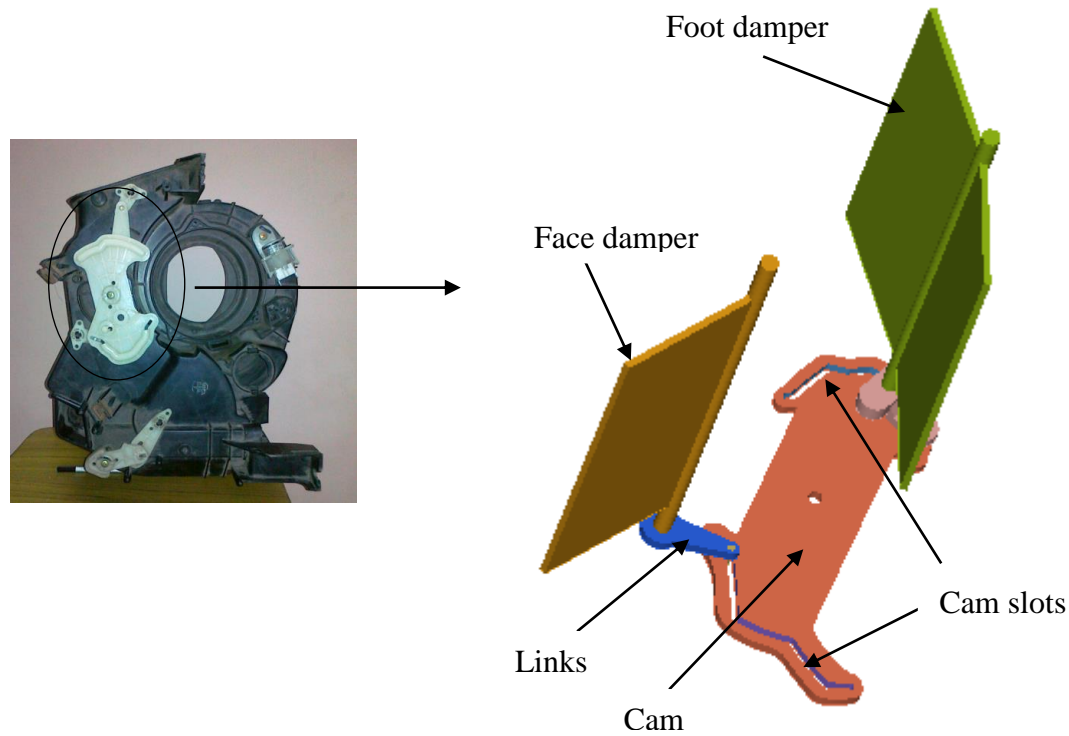


Figure 2.2: HVAC kinematic mechanism

It was found that the single lever configuration used in the design led to higher torque requirement along with more space requirement. Torque required in the two link configuration was lesser than in the current design, thus lowering the effort required to rotate the cam from the control panel.

C. Alexandru *et al.* [4] studied the functional optimization of Windshield wiper mechanisms.

The virtual model of the wiper system was made using the MBS package ADAMS of MSC Software. The functional optimization of the virtual model of a windshield wiper mechanism was done in the following sequence: the prototype was parameterized, design variables were defined, the design objective for optimization defined, parametric studies were performed, and the model was optimized on the basis of the main design variables.

Parametric study allows identifying the main design variables and having a great influence on the operational performance of the windshield wiper mechanism.

It was concluded that the approach of vehicle subsystems brings important advantages: it reduces time and cost of new product development. It also reduced the product cycles, the number of physical prototypes and offers more design alternatives. MBS-based design tools allow the engineer to operate the projected reductions in cycles, while maintaining or increasing performance, safety, and reliability of vehicles.

F. J. Espadafor *et al.* [5] analysed the failure of a crankshaft of a diesel engine.

They analysed a catastrophic crankshaft failure of a four-stroke 18 V diesel engine of a power plant for electrical generation when running at a nominal speed of 1500 rpm. The power of the engine was 1.5 MW and before failure it had accrued 20,000 hrs. in service functioning mainly at full load. The fracture happened in the web between the journal and the crankpin. The mechanical properties of the crankshaft containing tensile properties and surface hardness were evaluated. Fractographic studies showed that fatigue was the dominant mechanism of crankshaft failure, where the beach marks can be clearly identified. A thin and very hard zone was discovered in the template surface close to the fracture initiation point, which suggested that it was the origin of the fatigue fracture. A finite element model of the crankshaft predicted that the most heavily loaded areas match the fractured zone. The simulation model was composed of a dynamic lumped model linked to a finite element model. The analysis of the simulation results revealed different zones where the maximum stresses were reached, which could be considered to have the same failure probability, with the estimated stress level for fatigue initiation being in the range 260–275 MPa. One of these zones coincided with the zone where the fatigue failure originated and so it was well matched to the results of the material analyses. It was concluded that the failure was produced in one of the most stressed areas, where the material had abnormalities.

J. W. Yoon *et al.* [6] carried out the Fatigue analysis of the main frame of overhead transportation vehicles using flexible multibody dynamics.

The study analysed the fatigue life of an OHT main frame using a flexible multibody dynamic model. To predict the fatigue lives of parts, the calculation procedure required three kinds of data: Dynamic stress time history from a dynamic analysis, material properties of the components and stress curves of the parts. A flexible multibody model

was developed with the help of a finite element model and a multibody model. To ensure the reliability of the model, strain and displacement measurement tests were done. After the reliability verification, the fatigue life of the main frame was predicted.

The verified model was used to predict the dynamic behaviour of the vehicle on various railways operated according to a schedule, such as acceleration and deceleration and loading and unloading of freights. The main aluminium frame was translated into an FE model, and it was also verified by modal tests. According to the proposed procedures for fatigue life analysis were synthesized and analysed to predict the fatigue life. The fatigue life of the main frame was longer than the desired target life.

M. Machado *et al.* [7] studied the Dynamic response of multibody systems with 3D contact-impact events: influence of the contact force model.

Contact-impact events can frequently occur in the collision of two or more bodies that can be unconstrained or may belong to a multibody system. A study on the dynamic response of 3D multibody systems that experience contact-impact events is presented in this study, where different contact force models are used in order to check how the contact force law affects the dynamic behaviour of the whole system. It is concluded that all the contact force models exhibit a similar behaviour for high values of coefficient of restitution. For low values of the restitution coefficient, in the Flores *et al.* approach, the hysteresis damping factor increases asymptotically with the decrease of the coefficient of restitution, which can be considered to be a superior model for inelastic contacts.

M. Xingguo *et al.* [8] performed Multi-body Dynamics Simulation on Flexible Crankshaft System.

An effective prototype of flexible multi-body crankshaft system of engine was used for the dynamics Simulation. The dynamic boundary loads on the joints in a working cycle were determined by the simulation on the crankshaft system. The modelling of a effective prototype of crankshaft system had three steps. First, the three-dimensional model of these parts was built in modelling software. Second, they were transferred to ADAMS. Finally, the kinematical pairs were simplified to the ideal constraint used in the dynamics simulation. To consider the elastic deformation of crankshaft, a relative description method is adopted to create the flexible model of crankshaft, and then the motion of crankshaft can be disassembled as implication movement of rigid crankshaft and

deformation of flexible crankshaft relative to the moving reference frame. Modal analysis is achieved by ANSYS.

It was concluded that the flexible multi-body dynamics simulation was based on the crankshaft system or a effective prototype so it can simulate mechanical behaviour of crankshaft of engine in real working condition. Comparing with the common analysis method about individual crankshaft, this method had three advantages. Firstly, the system model was more approach to the physical prototype. Secondly, it needed fewer hypotheses. Thirdly, it faced to process rather than moment, thus this method had higher analysis precision.

N. Bertorelli *et al.* [9] performed structural crash analysis with ADAMS to make comparison between multibody and FEM approaches.

The work deals with modelling of mechanical structures subjected to impact loading with a multibody approach. The main purpose is to verify and evaluate the capabilities of the commercial rigid-body code ADAMS in order to analyse the deep plastic collapse behaviour of structural members. A simple model of a bending collapse of a thin walled rectangular cross section beam was considered. The model validation done by comparison with an analytical solution of a simple non-linear model solving the ordinary differential equation of motion of the system subjected to impulse load and the two solutions have been compared. The solution was obtained with two different approaches: a FEM analysis and a multibody analysis. The first one was performed by using an explicit integrator of the equation of motion, DYNA3D code, and the second one was solved with the ADAMS code. It was concluded from the study that ADAMS could be used successfully to study structural impact problems that involve large displacements and highly non-linear material behaviour. Global approach with ADAMS allowed the designer to obtain a good first-stage solution in a very short time, with a good confidence of results.

O. A. Bauchau and C. Ju [10] modelled the friction phenomena in flexible multibody dynamics.

They focused on the development of methodologies for the analysis of unilateral contact condition in joints and of the resulting normal and friction forces and calculated that the kinematics of the contacting bodies must be generalized so as to allow a variety of joint configurations to be considered. Robust schemes were used for numerical problem. Two joint configurations were developed, the planar and spatial clearance joints that can deal

with typical configurations where contact and clearance were likely to occur. The kinematic analysis of the joint yielded two important quantities: the relative distance between the bodies that drives the intermittent contact model and the relative tangential velocity that drives the friction model. This physics based model was capable of capturing a number of experimentally observed phenomena associated with friction. From a numerical stand point, it eliminated the discontinuity associated with Coulomb's friction law. Discretization was proposed for both normal contact and friction forces that implied an energy balance for the former and energy dissipation for the latter. When combined with the energy decaying schemes used in the effort, these properties of the discretization guaranteed the nonlinear stability of the overall numerical process. The numerical simulations relied on time step adaptively; simple, yet effective strategies were given to evaluate the required time step size when contact and friction were occurring. The efficiency of the proposed approach was demonstrated by realistic numerical examples that demonstrate the coupling between contact and friction forces and the overall dynamic response of the system.

P. Flores [11] performed Modeling and simulation of wear in revolute clearance joints in multibody systems.

The main goal of this work was to develop a methodology for studying and quantifying the wear phenomenon in revolute clearance joints. An approach was developed under the framework of a multibody systems formulation. The wear model used was based on the generalized Archard's equation, which relates the material volume loss with physical and geometrical properties of the contacting bodies. The wear approach was quite easy and straightforward to implement in a computational program. A simple four bar mechanism, which have a revolute joint with clearance, was used as an application of numerical example, to show the wear phenomenon and its behavior of global dynamics. From the main qualitative and quantitative results obtained, it was validated that the wear depth along the joint surface is non-uniform, due to the contact between the journal and bearing walls is wider and more frequent in some specific regions.

S. C. Jaiswal *et al.* [12] studied the multibody dynamic analysis and simulation of engine model.

This project studied the design and FE analysis of engine critical components from the base design of in house existing engine. Firstly the critical parts are made with the help of

3D modelling software. The input from proposed engine performance data, stress analysis was performed, which comprised power output, crank, piston assembly. The boundary condition of connecting rod and crankshaft are applied over the respective FE models and the processing part was done by OptiStruct.

The contour plot for stress and displacement was plotted. The different input velocities were taken at trial and error method. The graph plot for stress shows that there is no stress developed in any component of the engine at a particular given speed of 4mm/s. So the model was successful for that speed or less. Beyond this speed the stresses will develop and the model will fail. In case of cylinder block, the pre-processing part was finished and the boundary conditions are identified. The FE result was interpreted with the yield strength of the component material and FOS was calculated. The result of this analysis predicts the safer working of the parts under the stated operating condition.

S. H. Lee *et al.* [13] studied the Fatigue Life Analysis of Wheels on Guide way Vehicle using Multibody Dynamics.

The study analysed the fatigue life of the wheels in a guide way vehicle using a computational model and the wheel durability test. The dynamic stress time history of the wheels was estimated by using the quasi-static method, which applies linear superposition of the dynamic load time history obtained from multibody dynamic analysis and the static stress obtained from finite element analysis. The reliability of the multibody dynamics model was confirmed by comparison of the results from the model with the test result from the laser tracker. The material property of the wheels was obtained by comparing the compression displacement test results with the static analysis results and the static stress was analysed by using the finite element model and material property. The fatigue life of the wheels was estimated by using the S-N curve, which was obtained by the wheel fatigue test, and the dynamic stress time history, which was calculated by the computational model.

S. Magheri *et al.* [14] developed an innovative wheel–rail contact model for multibody applications.

In this work an innovative differential contact model was presented with the aim of achieving a better integration between multibody and differential modelling. The developed procedure required the discretization of the elastic contact problem and subsequently the solution of the nonlinear discrete problem. Both the steps were

implemented in the Matlab/Simulink environment. The contact model was inserted into a 2D multibody model of a railway vehicle to obtain a complete model of the wagon. The choice of 2D multibody model allows us to study lateral vehicle dynamics while reducing computational load. A 2D multibody model of the same vehicle was then assessed using Simpack Rail, which was a widely tested and validated by commercially available multibody software used for modelling railway vehicle behaviour. Finally numerical simulations of the vehicle dynamics was carried out on many different railway tracks with the aim of evaluating the performance of the entire model. The comparison between the results obtained by the Matlab model and those obtained by the Simpack Rail model has allowed an accurate and reliable validation of the new contact model. It was concluded that the performance of the Matlab model turned out to be good both in terms of output accuracy (kinematic variables, contact forces and contact patch) and in terms of numerical efficiency (performance of the numerical algorithms and time consumption).

S. Mukras *et al.* [15] analysed planar multibody systems with revolute joint.

They worked on the dynamic analysis of a planar multibody system with joint clearance. An analysis of multibody systems with revolute joint wear, which involves integrating wear prediction into the dynamic analysis, is discussed. The analysis procedure was then validated by modelling a slider-crank mechanism with single joint wearing and comparing the predictions with wear on an experimentally equivalent mechanism. The integrated model was used here to predict the wear occurring at the crank-follower joint of a slider-crank mechanism. Simulation results are compared to experimental data. This serves as both a demonstration of the integration model as well as a validation of the process. The goal of the experimental test was to determine the wear that occurs at the joint between the crank and follower after several thousand revolutions of the crank. It was concluded that the simulation closely predicts the reaction force except for some peaks that occurs at half crank rotation. These peaks were attributed to the direction change when the slider briefly impacts the sliding rail and resulting in the higher order dynamics. However, these peaks do not appreciably affected wear calculation because the sliding distance at this location was very small.

The above literature review shows that a lot of research in the area of kinematic and dynamic analysis of the different components of a vehicle has been done but very little

work has been found on Heating, Ventilating and Cooling (HVAC) module of an automotive air conditioning system.

Some of the gaps that have been found in the previous research work in this area are as follows:

- Effect on torque required to operate the cam by varying the speed of cam.
- Friction between the cam slots and pins has not been considered in the simulation of HVAC kinematics.
- The forces due to air flow on the dampers have not been taken into account and their effect studied.
- Analysis of the part by flexible body simulation.
- Stresses produced on the parts of the mechanism.

The present work is an attempt to take care of some of the aspects listed above, by incorporating them in the methodology proposed for the analysis of HVAC kinematics.

HVAC KINEMATIC MECHANISM SIMULATION

3.1 PROBLEM DEFINITION

Heating, Ventilating and Cooling (HVAC) module is a very important part of the automotive air conditioning system, shown in Fig.3.1. In order to control the air flow in various modes (foot, face, defrost) by the movement of doors / dampers, the kinematic mechanism is an integral part of any HVAC module. The design and validation of the HVAC kinematics is a crucial step in the design process of the complete module.

The design of the HVAC kinematic parts using CAD tools and the effort required to operate the cam can be explored by using the virtual simulation CAE tools. A study of Multibody dynamics systems and the simulation techniques has been made, which is used for the proposed work.

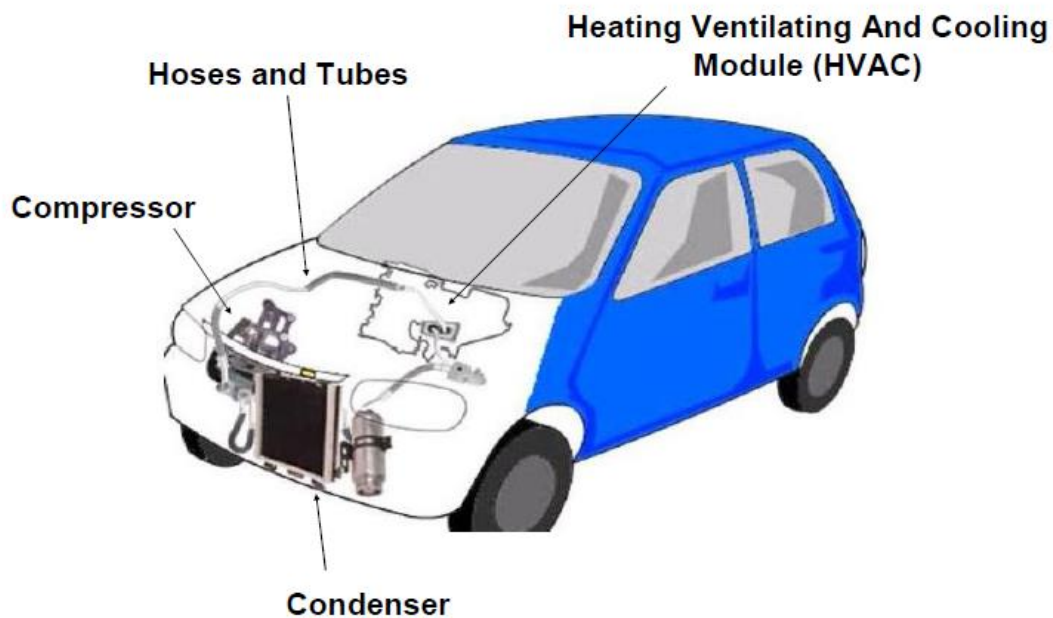


Figure 3.1: Components of car AC system

3.2 INTRODUCTION TO HVAC KINEMATIC MECHANISM

An automotive air-conditioning system has an HVAC module mounted on the firewall of the vehicle. The HVAC module consists of various parts like heater, evaporator, blower, doors/dampers, levers, cams, etc. All these parts are placed in plastic cases, and the final assembly is mounted in the vehicle. The air blown by the blower passes through the evaporator and/or the heater located inside the HVAC module and is thus cooled and/or heated up accordingly. There are openings provided in the cases for airflow in various modes. Five different modes are face, foot, bi-level (face/foot), defrost and foot/defrost. The HVAC module has a mechanism consisting of various links and a cam responsible for controlling the air flow going through these modes to the passenger cabin. The calculation of displacement and torque for these modes is a major challenge while designing the kinematics mechanism for an HVAC module. The torque required to operate the cam should not be very high, as this would lead to passenger discomfort while using the various knobs on the control panel in the vehicle. The HVAC module parts considered for the analysis are Cam, Links, Foot damper, Face damper as shown in Fig.3.2.

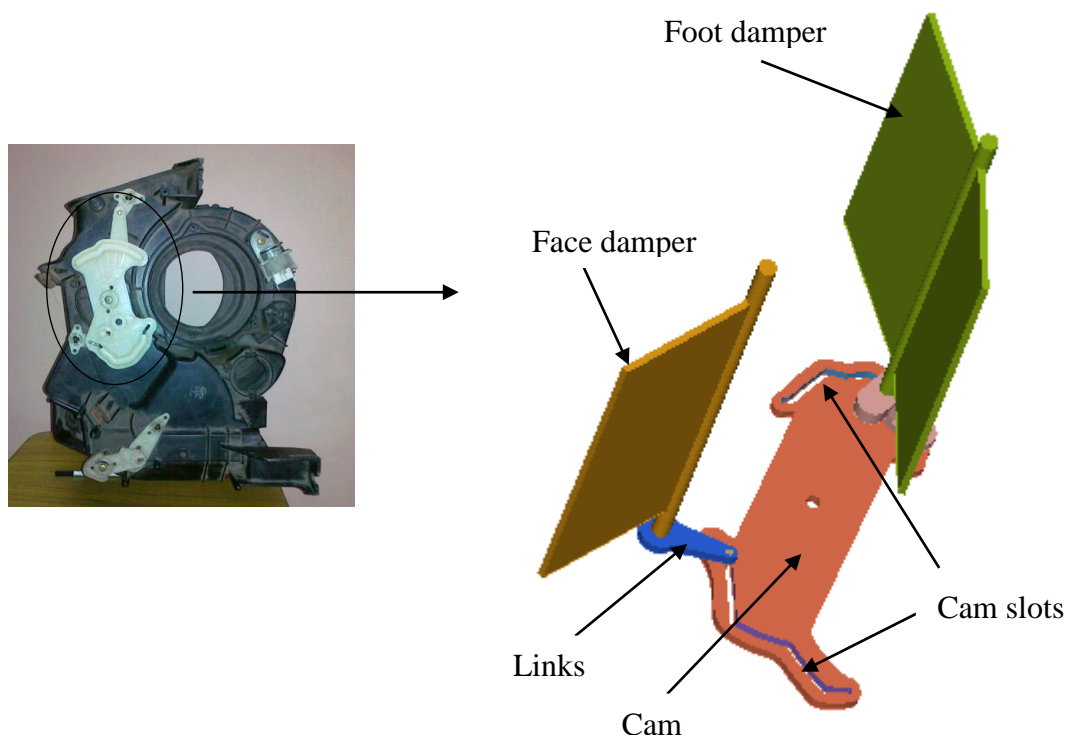


Figure 3.2: HVAC kinematic mechanism

3.3 DESIGN AND ANALYSIS CYCLE OF HVAC

The present section briefly summarizes some of the details of the background information needed for the kinematics analysis, conducted for the HVAC module using CAE software.

The complete design and analysis cycle requires:

- [1] Design of internal parts of HVAC module such as dampers, plastic cases, etc.
- [2] Kinematics design of HVAC mechanism.

The following are the major steps for the design and analysis of the HVAC mechanism:

1. The layout design of all the internal HVAC parts is done on the basis of packaging space available in the vehicle, and the A/C system selection based on the heat load calculations.
2. Based upon this, the location, layout and design of dampers are finalized.
3. The customer data for air flow distribution and the CAD parts (HVAC cases and dampers) are given for CFD analysis, which provides the damper angles for proper air flow in various modes.
4. Based on the CFD input, the damper angles are finalized and the other parts like levers, cam, rods, etc. are designed.
5. CAE Software is used for calculation of displacement and torque values required to operate the kinematics parts, and the results are compared with the input data for the validation of design.

The HVAC kinematic mechanism simulation (step 5) in the design and analysis cycle of HVAC is discussed in detail in the following sections.

3.4 KINEMATIC ANALYSIS OF HVAC MECHANISM

The details of the kinematics analysis done for the HVAC mechanism are discussed in this section. The following steps are used to create the mechanism model, conduct the analysis and generate the results for the HVAC mechanism.

- a) Reverse engineering data of HVAC components
- b) CAD model of the assembly.
- c) Mass and inertial properties of the various parts in the mechanism

- d) Discretization of the CAD geometry.
- e) Pre-processing.
- f) Solution
- g) Post processing

All the steps are described in detail below-:

3.4.1 Reverse Engineering of HVAC Components

The Reverse engineering of HVAC unit is done with the help of different instruments. The major problem during the reverse engineering process was to measure the cam slots. Measurement was done by tracing the slots on a paper. Then number of points, about 90, were marked over the traced slot and the x and y coordinates of these points with respect to a reference frame were noted down. This coordinate data was entered into the CAD software and the points were joined by splines to make the slot profile.

Fig.3.3 and 3.4 shows different points joined with the help of splines to make the slot profiles.

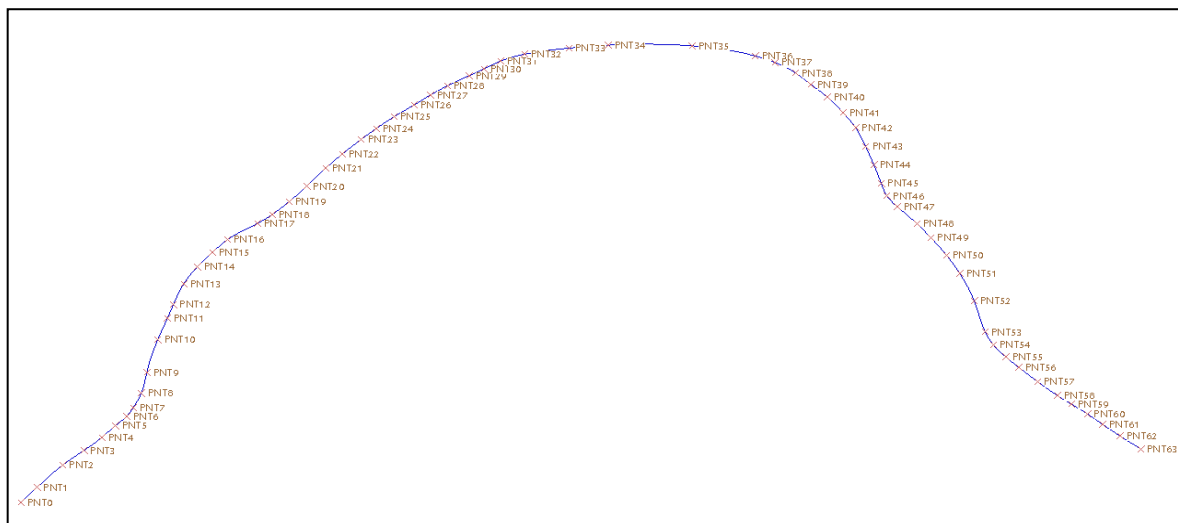


Figure 3.3: Slot 1 Profile

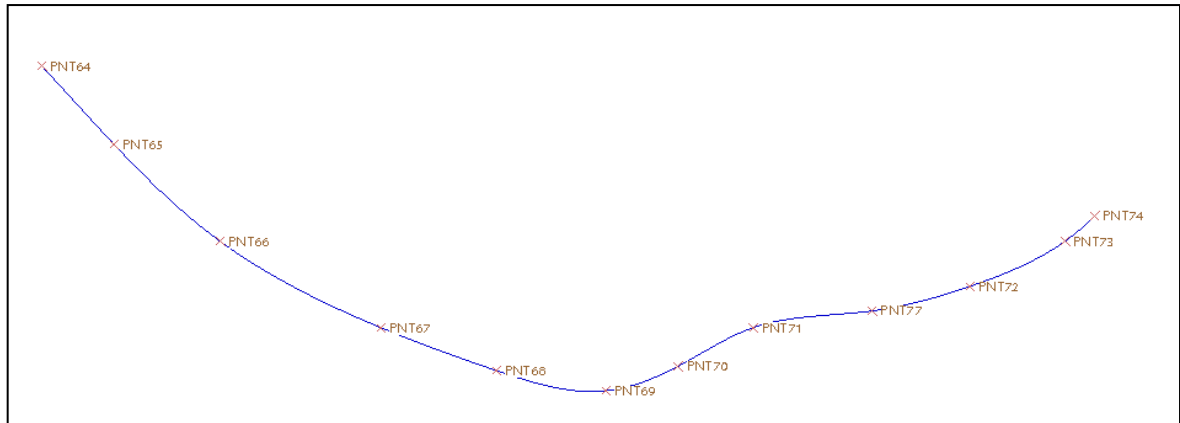


Figure 3.4: Slot 2 Profile

3.4.2 CAD Modelling of HVAC Components

All the components are modelled in Pro-E Wildfire 5 from the reverse engineered data. Critical work during the modelling was the exact location of all the components in the assembly, small error in the assembly may lead to large error in the kinematic movement of components. The exploded view of the assembly is shown in Fig.3.5.

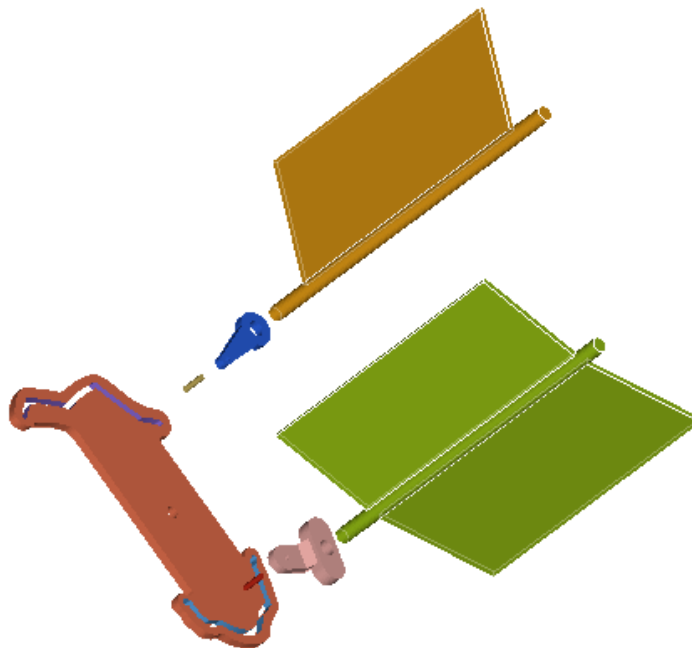


Figure 3.5: Exploded view of the assembly

3.4.3 Mass and Inertia Properties of HVAC Components

Mass and inertia properties of all the components are needed as an input data in the multibody analysis. Steel properties are assigned to the pins and PVC (plastic) properties

are assigned to the rest of components. Units are taken in $mm - kg - s$ system. The density of steel is taken $7.8270820 \times 10^{-6} \text{ kg/mm}^3$ and $1.3999833 \times 10^{-6} \text{ kg/mm}^3$ for PVC. Mass, Centre of gravity and inertial properties were extracted from the Pro-e assembly model of HVAC with respect to the fixed global frame.

3.4.4 Discretization of CAD Geometry

The CAD parts in the assembly are imported in CAE Software in the Initial Graphics Exchange Specification (IGES) format. The different parts are meshed using triangular elements. A fine mesh is used for the contact surfaces, which are placed in a different collector/group, and the rest of the surfaces are meshed coarse. Fine meshing of cam slot and pin is shown in Fig.3.6.

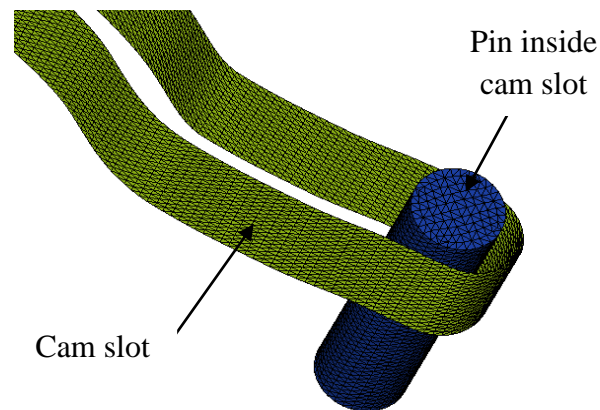
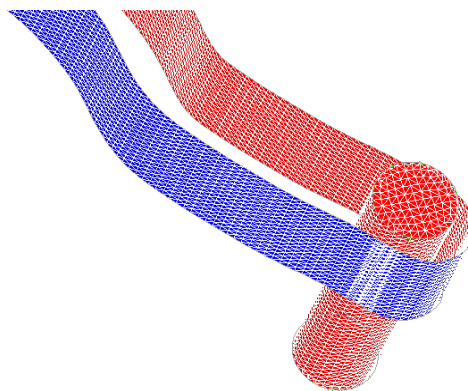


Figure 3.6: Fine meshing done to pins and cam slots



**Figure 3.7: Normal vectors of contact surfaces face each other
(Red colour shows the direction of normal vectors)**

The direction of the normal vectors of the elements used in contacts is of particular importance. The normal vectors of the surfaces coming in contact should face each other. Fig.3.7 shows the direction of normal vectors. Element size used for meshing pins and cam slots are 0.3 mm and 1 mm for the rest of the components. Meshing is done by using different component collectors to facilitate defining contacts between pins and cam slots and to facilitate attaching graphics to the respective bodies.

3.4.5 Pre- Processing

Points

Points are needed to define the centre of gravity locations of objects and joint locations. Seven points are created to define the centre of gravity of all the seven components and the various joints locations of HVAC. These cg points will be further used to define bodies. Centre of gravity locations of components are taken from CAD software (Pro-E). Coordinates of all the points are shown in Table 3.1.

Table 3.1: Coordinate data

	X	Y	Z
The Model			
Global Origin	0.000	0.000	0.000
cg_cam	59.973	2.500	-91.887
cg_link1	72.420	-8.003	-151.341
cg_pin1	58.247	0.500	-146.712
cg_link2	77.339	-3.500	-22.907
cg_pin2	65.219	0.500	-5.901
cg_door1	83.615	-112.832	-154.631
cg_door2	110.932	-108.500	-32.091
d1_b1	77.211	-9.000	-152.906
d1_b2	77.211	-206.000	-152.906
d2_b1	82.765	-5.500	-30.518
d2_b2	82.765	-209.500	-30.518
pin1_fix	58.247	-3.000	-146.712
pin2_fix	65.219	-3.000	-5.901
cam_cntr	58.190	3.000	-97.226

Bodies

Bodies are defined at different centre of gravity points using the mass and inertial properties extracted from the CAD software. Seven bodies are defined using the mass and inertial properties extracted from the CAD software. Mass and inertia properties of all the bodies are shown in Table 3.2.

Table 3.2: Mass and inertia properties

	Mass	bx	lyy	lzz	bxy	lzx	lyz
The Model							
Ground Body	0.000	0.000	0.000	0.000	0.000	0.000	0.000
Body_cam	0.051	77.903	113.634	35.941	0.000	-37.846	0.000
Body_link1	0.006	0.476	0.859	0.542	0.127	0.024	-0.042
Body_pin1	0.001	0.011	0.001	0.011	0.000	0.000	0.000
Body_link2	0.003	0.256	0.399	0.155	0.000	0.147	0.000
Body_pin2	0.001	0.011	0.001	0.011	0.000	0.000	0.000
Body_door1	0.108	363.740	150.675	313.216	0.462	69.874	-0.124
Body_door2	0.064	169.356	33.730	202.672	0.000	1.866	0.000

The points and bodies created in the CAE Software are shown in Fig.3.8.

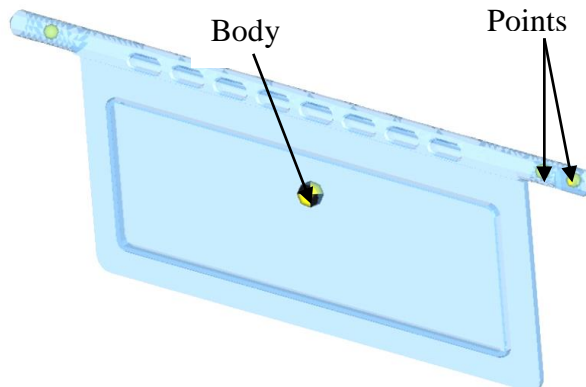


Figure 3.8: Points and bodies created

Joints

Joints are defined to constrain the motion of the mechanism, three types of joints are used in the analysis setup these are revolute joint, fixed joint and ball joint. To define a joint we need two bodies between which the joint is needed, a common point and the type of joint. In the pre-processing 9 joints are defined.

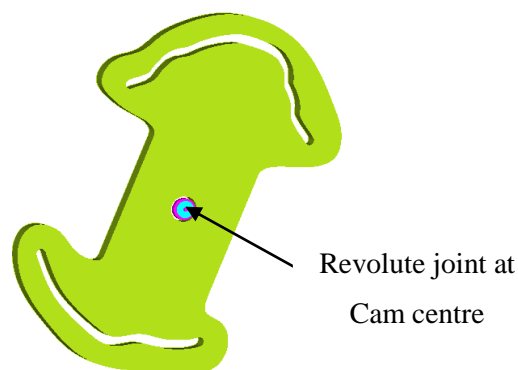


Figure 3.9: Joints created

Four ball joints are provided at the bearing locations where the dampers are supported. Fixed joints are defined to attach the links to the dampers. Pins are fixed to the links by fixed joints. Revolute joints are provided at the cam centre and ground to facilitate the rotation. Fig.3.9 shows the revolute joint created at the cam centre.

The various joints defined in the analysis setup are:

1. Revolute joint between the cam and ground (cam_revo).
2. Ball joint 1 between face damper and ground (d1_b1).
3. Ball joint 2 between face damper and ground (d1_b2).
4. Ball joint 1 between foot damper and ground (d2_b1).
5. Ball joint 2 between foot damper and ground (d2_b2).
6. Fixed joint between link1 and door1 (link1_fix).
7. Fixed joint between link2 and door2 (link2_fix).
8. Fixed joint between link1 and pin1 (pin1_fix).
9. Fixed joint between link2 and pin2 (pin2_fix).

Contact

Contacts are defined between the cam slots and the portion of the lever pin outer surface as shown in Fig.3.10. A suitable value of penalty (3000) and restitution coefficient (0.05) is given for the contacts. Friction is not taken into consideration, as it increases the complexity of the model and thus, the solver time. The penalty value determines the local stiffness properties between the materials. Larger values lead to reduced penetration between two bodies. The coefficient of restitution represents the energy loss between two bodies in contact. A value of 1 represents no energy loss and a perfectly elastic contact.

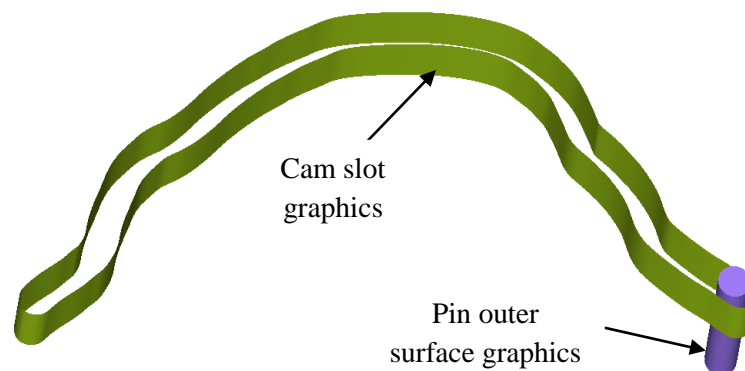


Figure 3.10: Graphics for contact

Graphics are needed to define contact between bodies as the meshing was done using different collectors we have graphics of slot1 and slot2 independently.

The various contacts defined are:

1. Poisson Contact between slot1 and pin1 (slot1_pin1).
2. Poisson Contact between slot2 and pin2 (slot2_pin2).

Motion

Initial motion is required to simulate the model, after defining all the joints a rotational motion of $10^\circ/\text{sec}$ is defined at the cam revolute joint using the expression “ $10D \times \text{TIME}$ ”. With this expression if the analysis is run for 5 seconds then the cam will rotate through 50° .

Outputs

Outputs are defined for cam rotation, doors rotation and torque required to operate the cam. Markers are required to define outputs. A marker is a coordinate system attached to a body that is used as a reference for applied loads and output requests. To define a marker, things to be specified are the associated body, the origin of the marker, and the axes' rules for the marker. Six markers are defined to produce the required outputs:

1. Marker defined at a point on rotational axis of cam with ground body (cam_ground).
2. Marker defined at a point on rotational axis of cam with cam body (cam_body).
3. Marker defined at a point on the rotational axis of face damper with ground body (d1_ground).
4. Marker defined at a point on the rotational axis of face damper with face damper body (door1).
5. Marker defined at a point on the rotational axis of foot damper with ground body (d2_ground).
6. Marker defined at a point on the rotational axis of foot damper with foot damper body (door2).

With these markers taken as reference, four outputs are defined for cam torque, cam rotation, door 1 rotation and door 2 rotations. For the rotational output of cam and doors expression ‘ $\text{AY}(\{\text{id string of ground body marker}\},\{\text{id string of component body marker}\}) * \text{rtod}$ ’ has been used. In the expression “AY” denotes angular output about global Y axis. As on each point on the rotational axis two markers has been defined one

with ground body and other with component body, in the braces the id strings of these two markers are taken. In expression “rtod” denotes conversion of degrees into radians.

1. Output defined for cam torque (cam_torque).
2. Output defined for cam rotation (cam_rot).
3. Output defined for foot damper rotation (door1_rot).
4. Output defined for face damper rotation (door2_rot).

After doing the pre-processing and resolving the errors the model is submitted for the Multibody analysis.

3.4.6 Solution

The solver is run for an end time of 8s, using the ABAM integrator type, and the outputs obtained are plotted in graph. The workstation used for the analysis has 3960 MB RAM, and a CPU speed of 2530 MHz.

3.4.7 Post Processing

The following outputs are obtained for HVAC kinematic mechanism:

- (a) Foot damper rotation as a function of cam rotation.
- (b) Face damper rotation as a function of cam rotation.
- (c) Torque as a function of cam rotation.

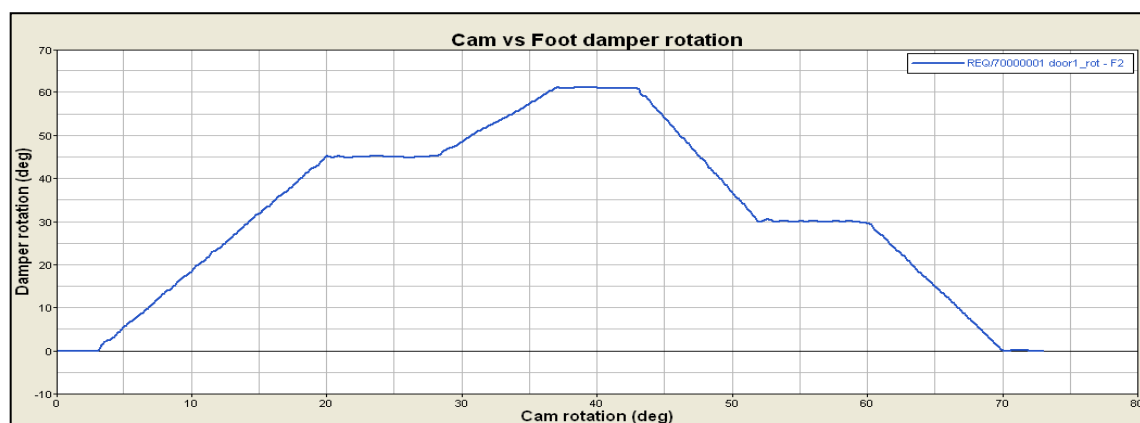


Figure 3.11: Cam vs. Foot damper rotation

As can be seen from Fig.3.11 and 3.12, there is an optimal level of door rotation for a given cam rotation angle. The door rotation should not be very high (as it will lead to high torque values) or very low, because sufficient level of air flows in a given time could not be achieved.

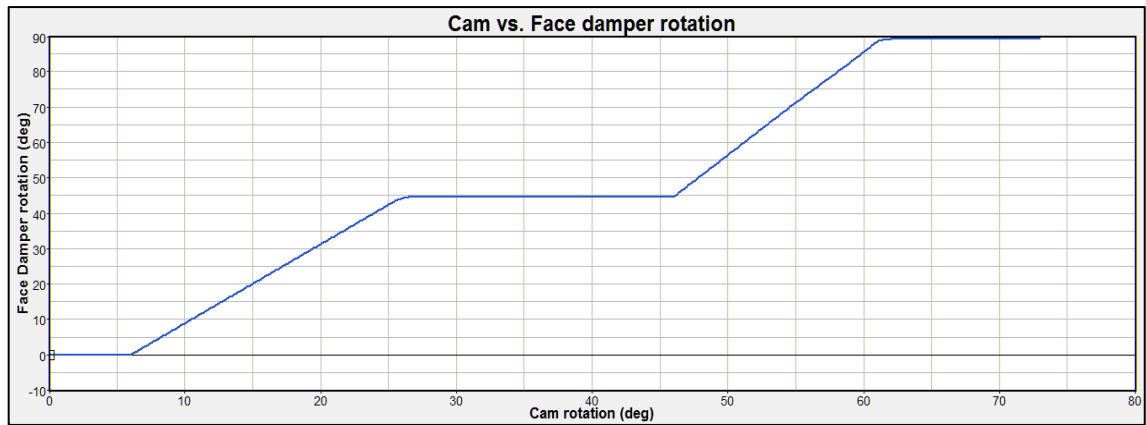


Figure 3.12: Cam vs. Face damper rotation

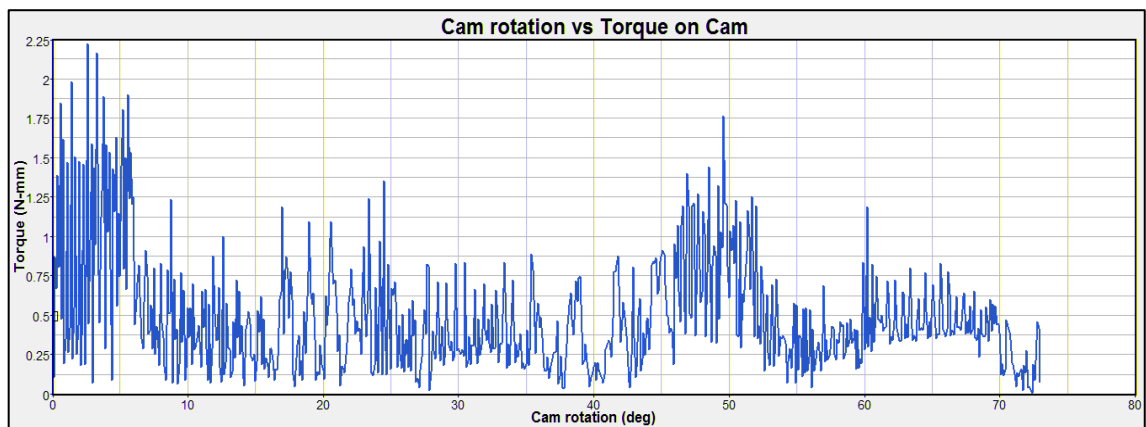


Figure 3.13: Cam rotation vs. Torque on cam

As can be seen from Fig.3.13, there are spikes in the torque graph because the cam slots are not so smooth due to the reverse engineering of the cam.

4.1 INTRODUCTION

HVAC kinematic mechanism design is one of the crucial steps in the design process of the complete module. Design should be compact and torque required to operate the cam should not be high. Base radius of the cam in the mechanism should be taken according to the space available. For the desired output results two mechanisms have been designed for the same dampers location and a comparison is made between the two designs. The assumptions include a constant angular velocity of the cam, and the rigidity of the parts in the mechanism. The movements of various parts have been analysed using the animation. The other important outputs include the cam rotation and torque on cam graphs plotted with the help of CAE Software.

The HVAC mechanism is designed of two types:

1. Single link mechanism
2. Double link mechanism

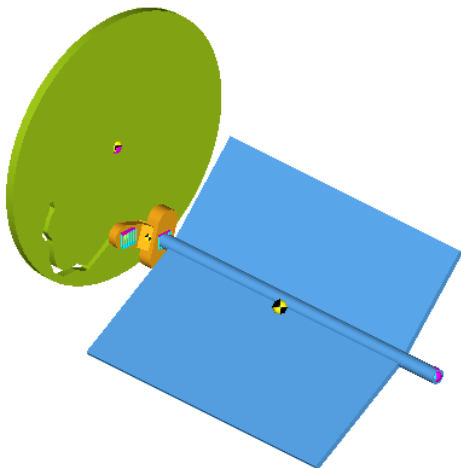


Fig 4.1 Single link mechanism

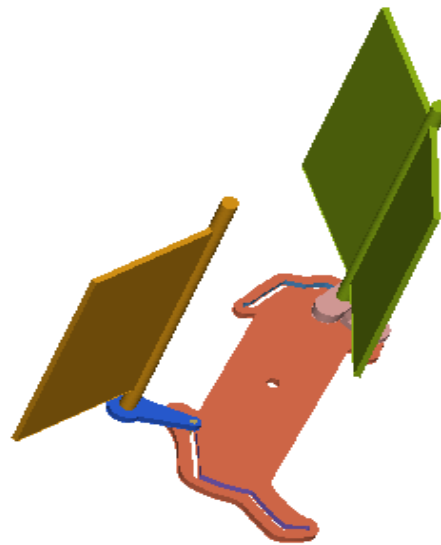


Fig 4.2 Double link mechanism

4.2 PRE-PROCESSING

Motion is given at revolute joint between ground body and cam at cam centre point. The simulations are done by varying the speed of cam so that the torque on cam can be analysed at different speeds. For the desired output results, cam rotation vs. torque on cam graphs is plotted. The results are obtained for the 73° rotation of the cam.

Initial motion is required to simulate the model, after defining all the joints a rotational motion is defined at the cam revolute joint using the expression “10D × TIME”. With this expression if the analysis is run for 5 seconds then the cam will rotate through 50°.

4.3 RESULTS

The outputs obtained by single link mechanism model are:

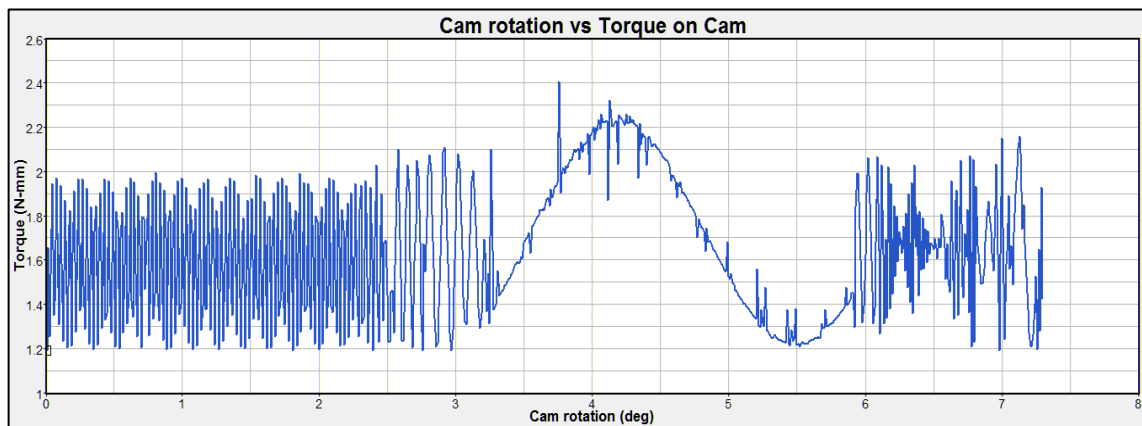


Figure 4.3: Cam rotation vs. Torque on cam at speed 1°/sec

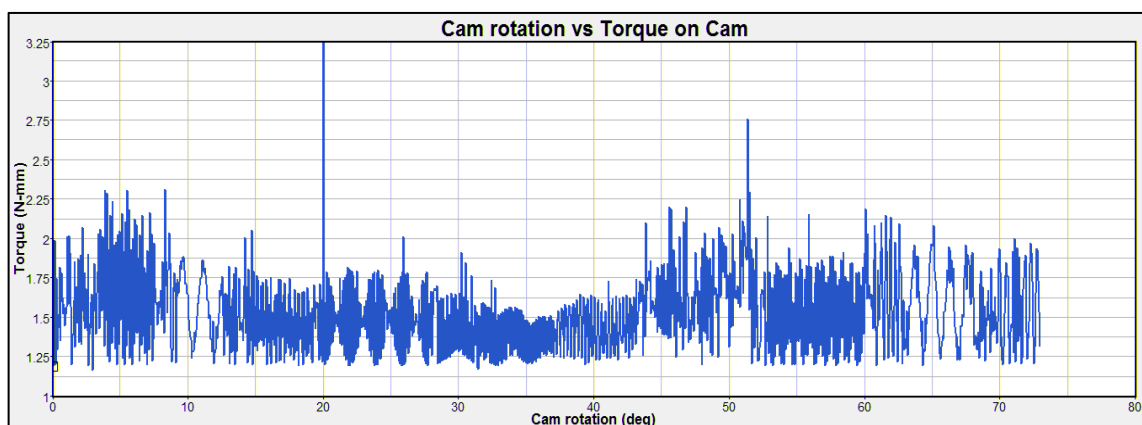


Figure 4.4: Cam rotation vs. Torque on cam at speed 5°/sec

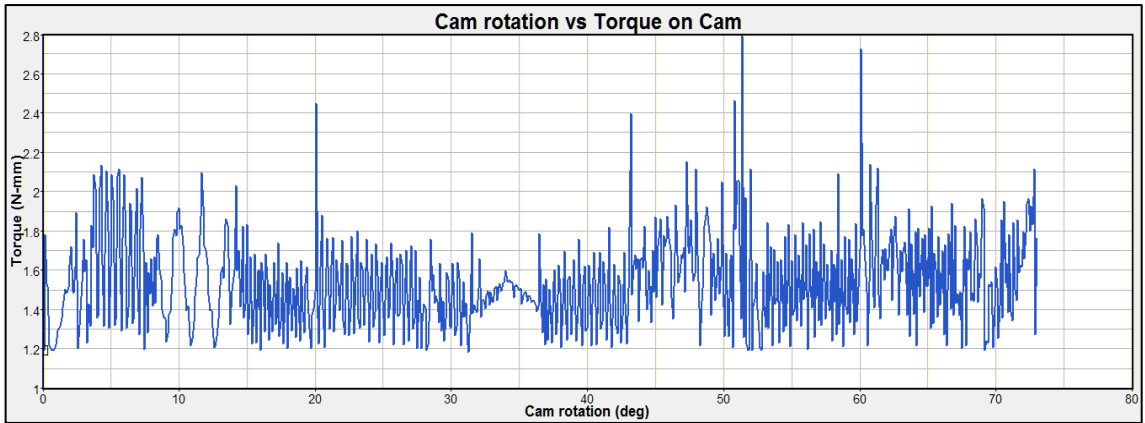


Figure 4.5: Cam rotation vs. Torque on cam at speed 10°/sec

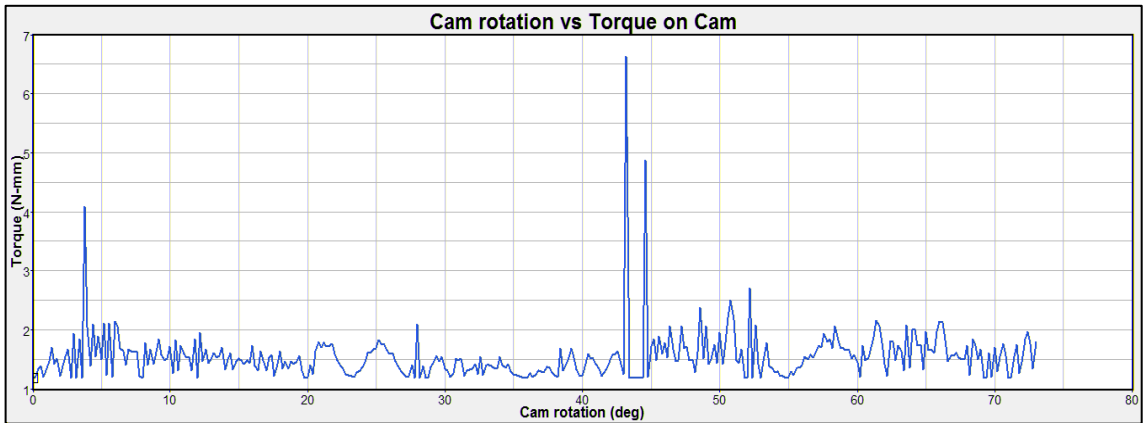


Figure 4.6: Cam rotation vs. Torque on cam at speed 20°/sec

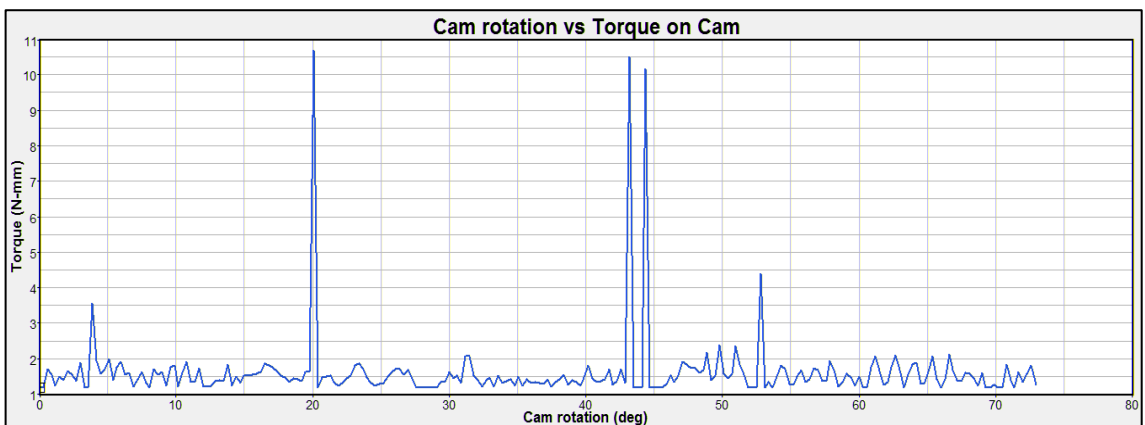


Figure 4.7: Cam rotation vs. Torque on cam at speed 30°/sec

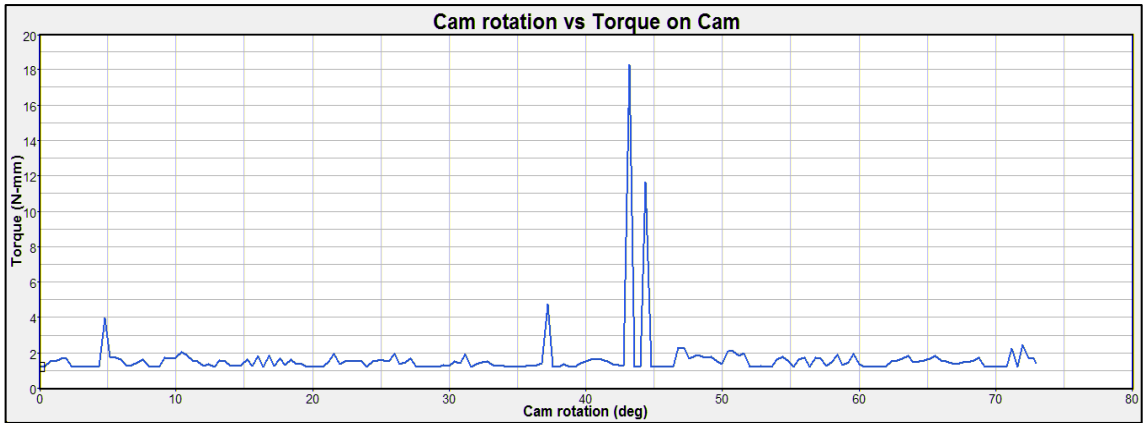


Figure 4.8: Cam rotation vs. Torque on cam at speed 40°/sec

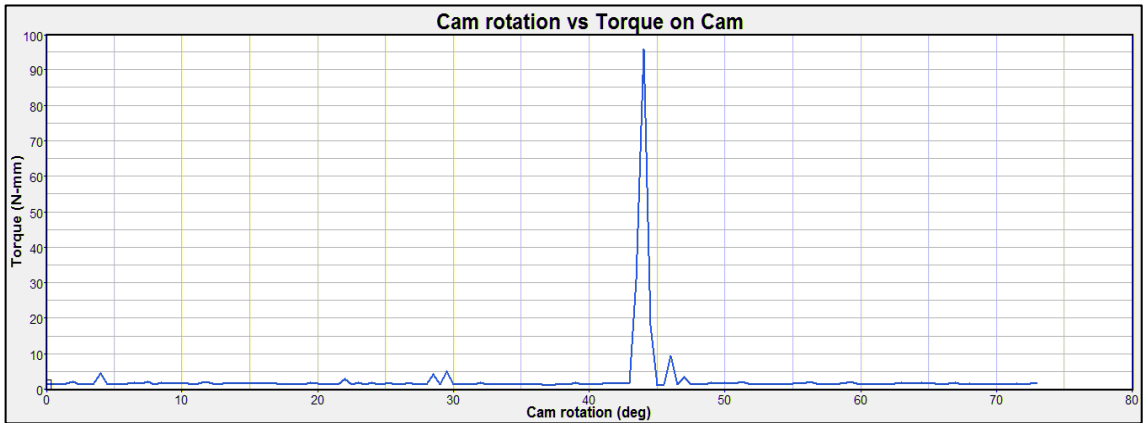


Figure 4.9: Cam rotation vs. Torque on cam at speed 50°/sec

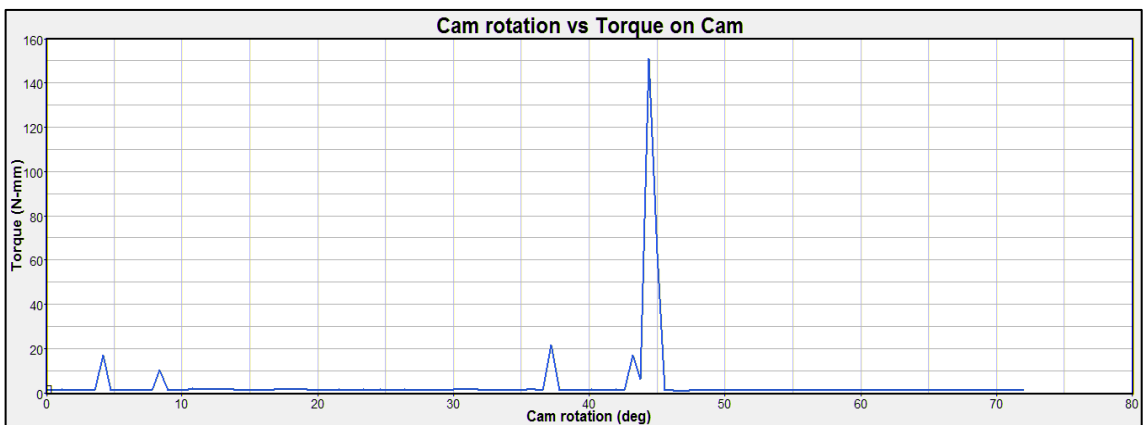


Figure 4.10: Cam rotation vs. Torque on cam at speed 60°/sec

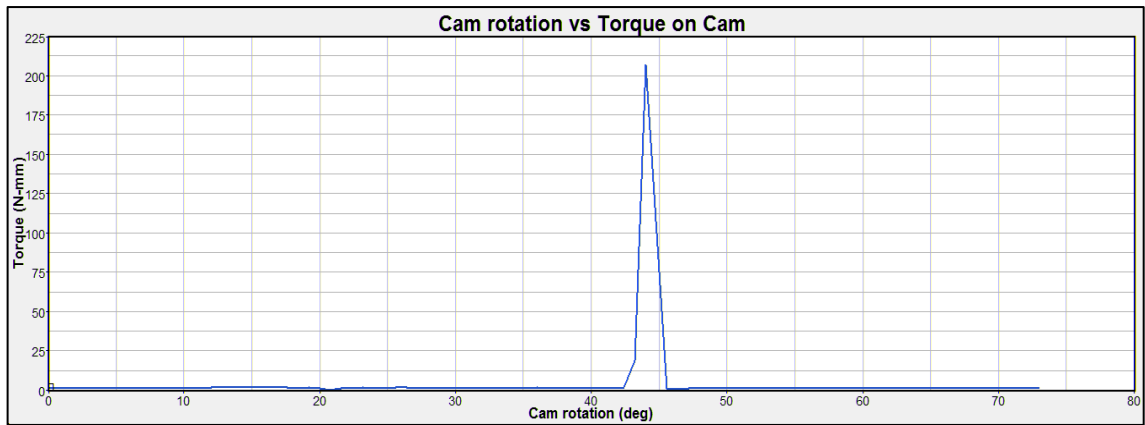


Figure 4.11: Cam rotation vs. Torque on cam at speed 80°/sec

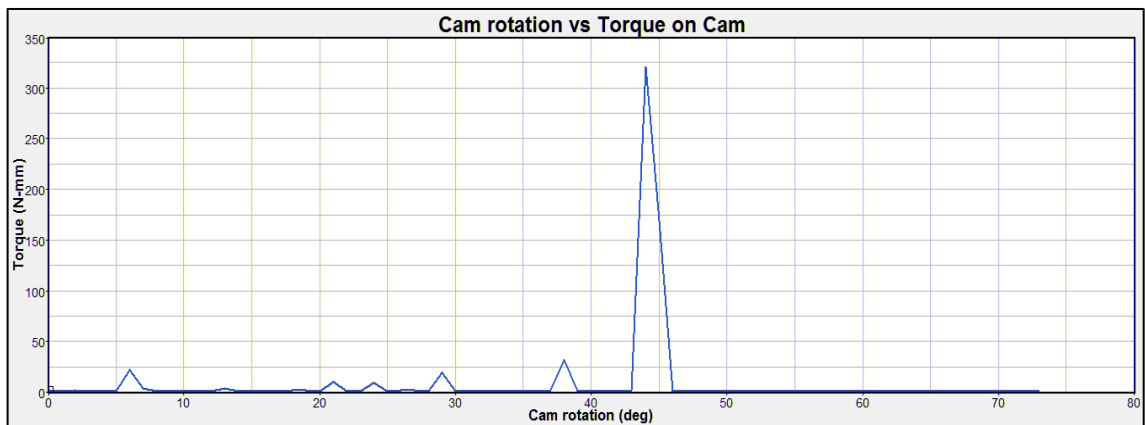


Figure 4.12: Cam rotation vs. Torque on cam at speed 100°/sec

The outputs obtained by double link mechanism model are:

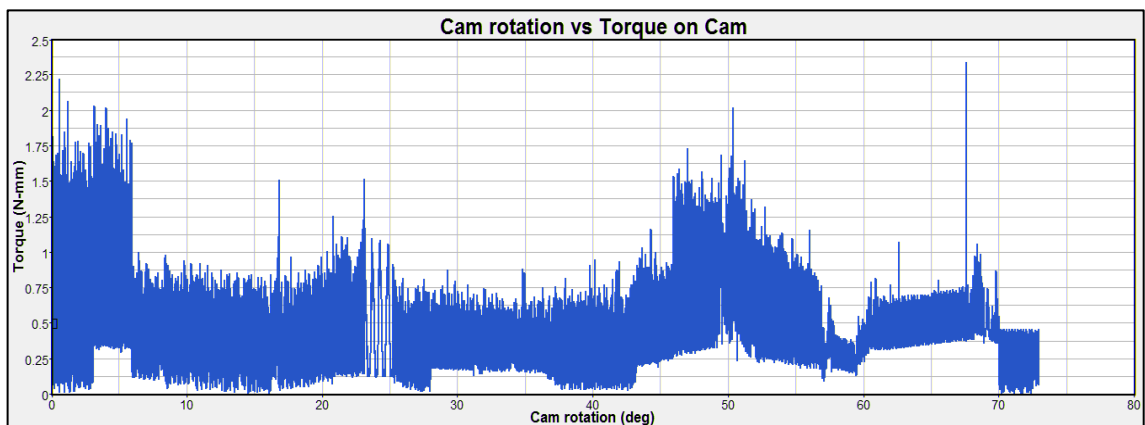


Figure 4.13: Cam rotation vs. Torque on cam at speed 1°/sec

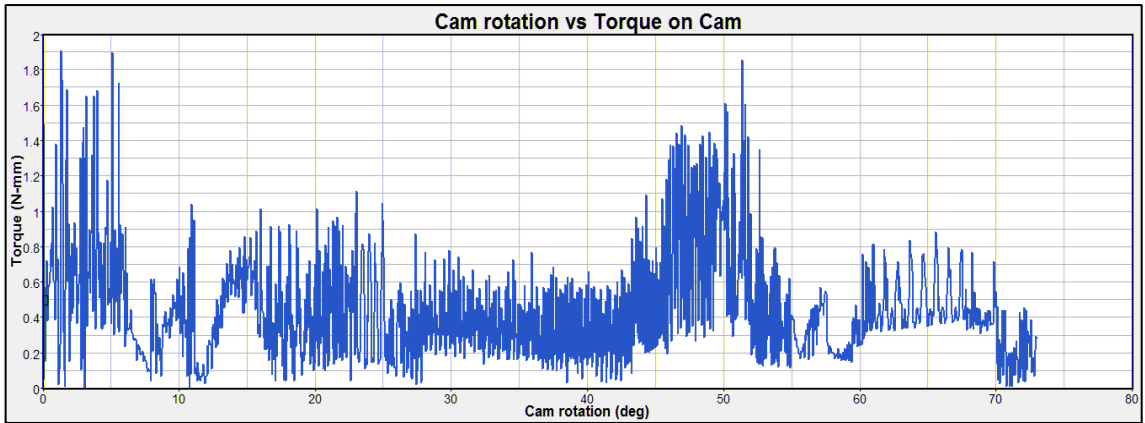


Figure 4.14: Cam rotation vs. Torque on cam at speed 5°/sec

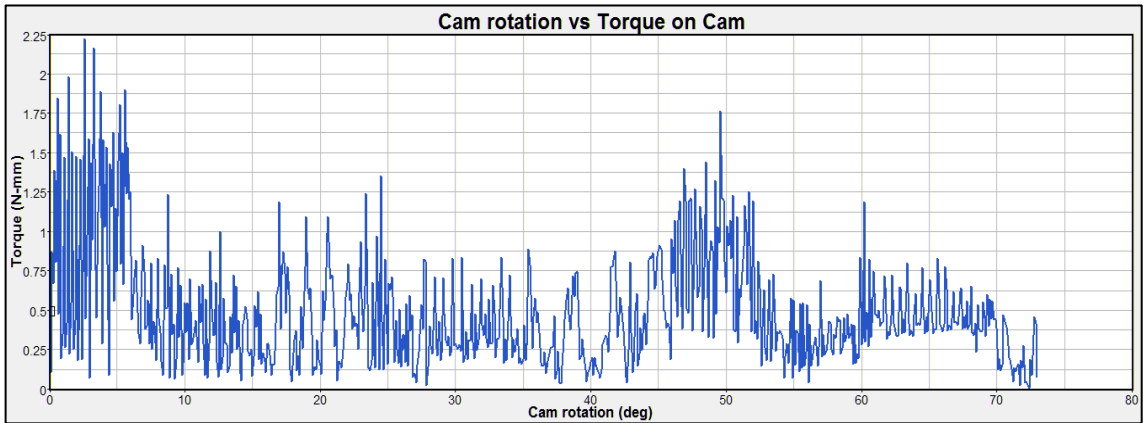


Figure 4.15: Cam rotation vs. Torque on cam at speed 10°/sec

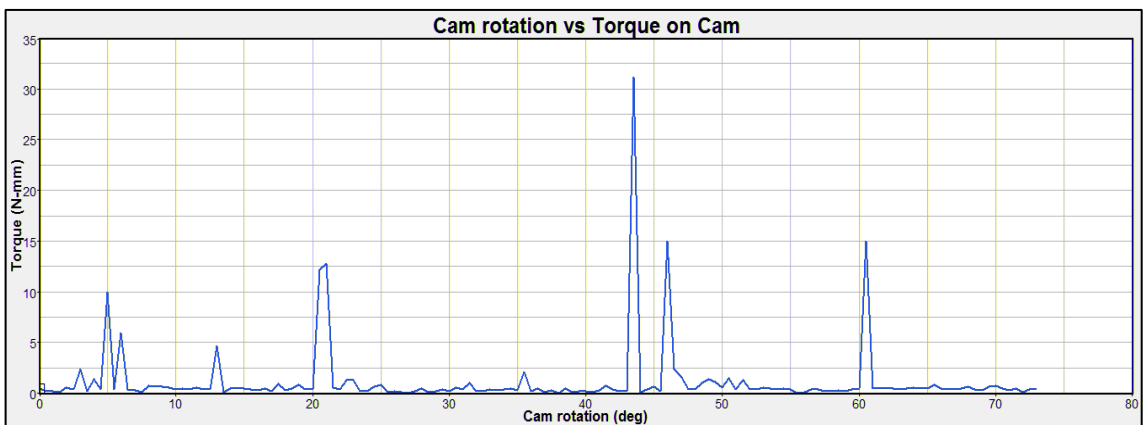


Figure 4.16: Cam rotation vs. Torque on cam at speed 50°/sec

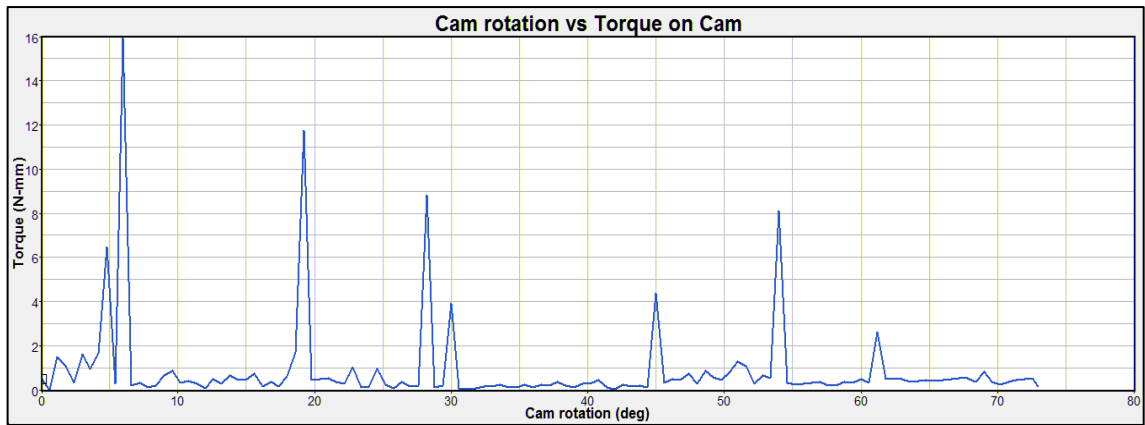


Figure 4.17: Cam rotation vs. Torque on cam at speed 60°/sec

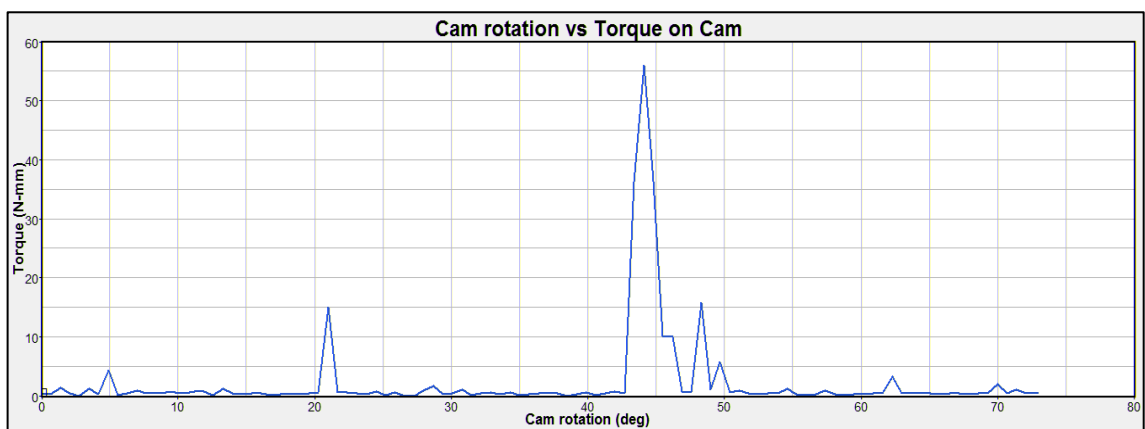


Figure 4.18: Cam rotation vs. Torque on cam at speed 70°/sec

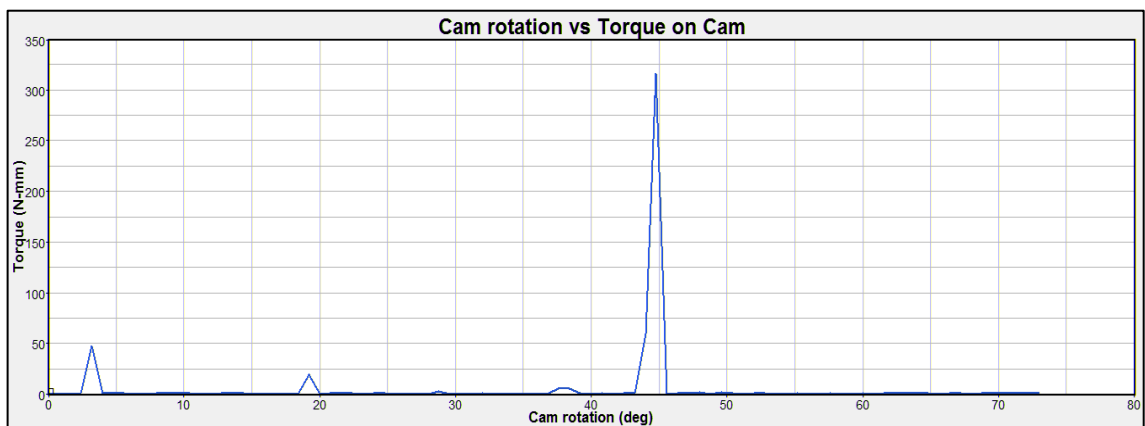


Figure 4.19: Cam rotation vs. Torque on cam at speed 80°/sec

With the help of above result, it is concluded that the torque on cam is increase by increasing the speed of cam.

5.1 INTRODUCTION

Contacts are defined between the cam slots and the lever pin outer surface as shown in Fig.5.1. A suitable value of penalty (3000) and restitution coefficient (0.05) is given for the contacts. The penalty value determines the local stiffness properties between the materials. Larger values lead to reduced penetration between two bodies. The coefficient of restitution represents the energy loss between two bodies in contact. A value of 1 represents no energy loss and a perfectly elastic contact. Graphics are needed to define contact between bodies as the meshing was done using different collectors. Poisson Contact between slot and pin is defined.

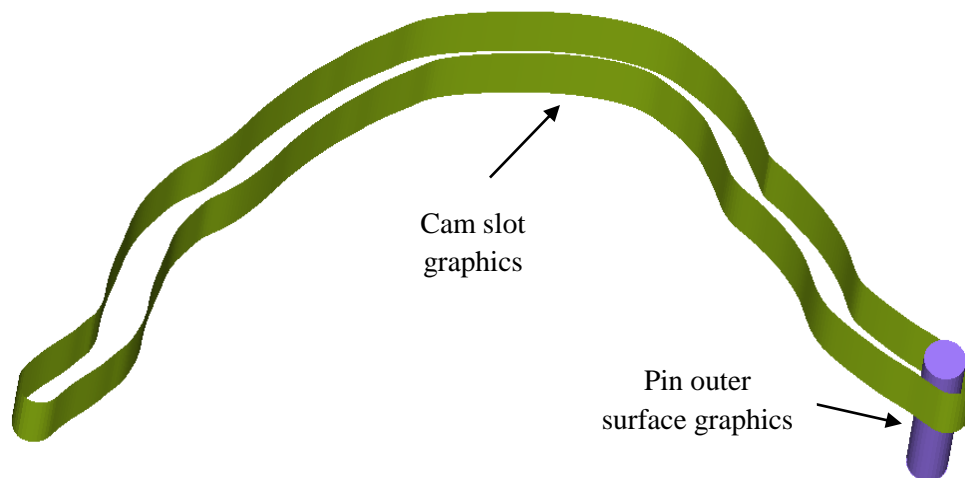


Figure 5.1: Slot and Pin Graphics

Friction between cam slot and pin is defined in contact definition between them. Pin is made of steel and cam material is PVC. The material properties are defined as discussed earlier. The coefficient of friction between two materials in relative sliding may depend on contact pressure, surface roughness of the relative harder contact surface, temperature, sliding velocity and the type of lubricant.

The coefficient of friction between metal and plastic are obtained from fig. 5.2. The static friction coefficient is 0.25 to 0.4 and the dynamic friction coefficient is 0.1 to 0.3.

Coefficient of friction for a range of material combinations				
combination	Static		Dynamic	
	dry	lubricated	dry	lubricated
steel-steel	0.5...0.6	0.15	0.4...0.6	0.15
copper-steel	-	-	0.5...0.8	0.15
steel-cast iron	0.2	0.1	0.2	0.05
cast iron - cast iron	0.25	0.15	0.2	0.15
friction material - steel	-	-	0.5-0.6	-
steel-ice	0.03	-	0.015	-
steel-wood	0.5-0.6	0.1	0.2-0.5	0.05
wood-wood	0.4-0.6	0.15...0.2	0.2...0.4	0.15
leather-metal	0.6	0.2	0.2...0.25	0.12
rubber-metal	1	-	0.5	-
plastic-metal	0.25...0.4	-	0.1...0.3	0.04...0.1
plastic-plastic	0.3-0.4	-	0.2...0.4	0.04...0.1

Figure 5.2: Coefficient of friction

The analyses are done at the constant speed of 10°/sec and the output results are obtained by incorporating the values of Static Friction coefficient (S) and Dynamic friction coefficient (D).

5.2 RESULTS

The results obtained for single link mechanism are shown in fig 5.3 to fig 5.7.

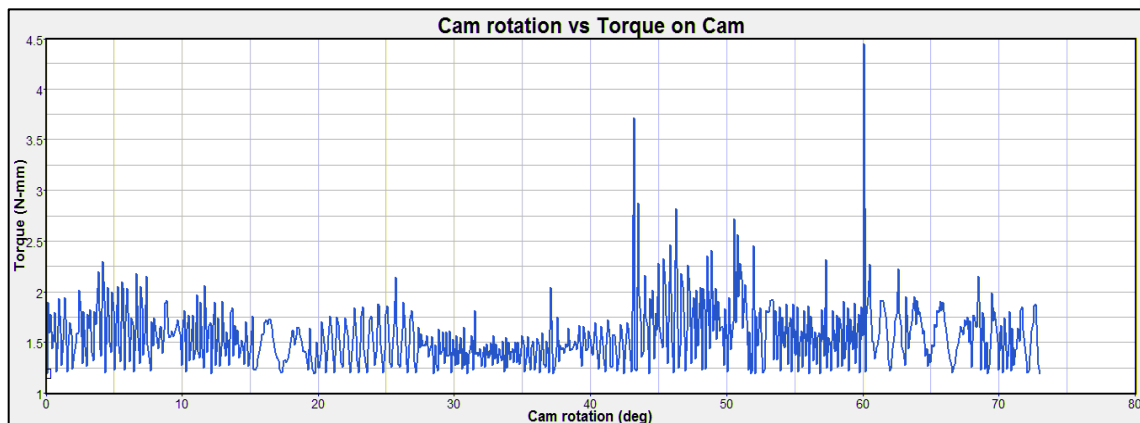


Figure 5.3: Cam rotation vs. Torque on cam at S=0.25, D=0.1

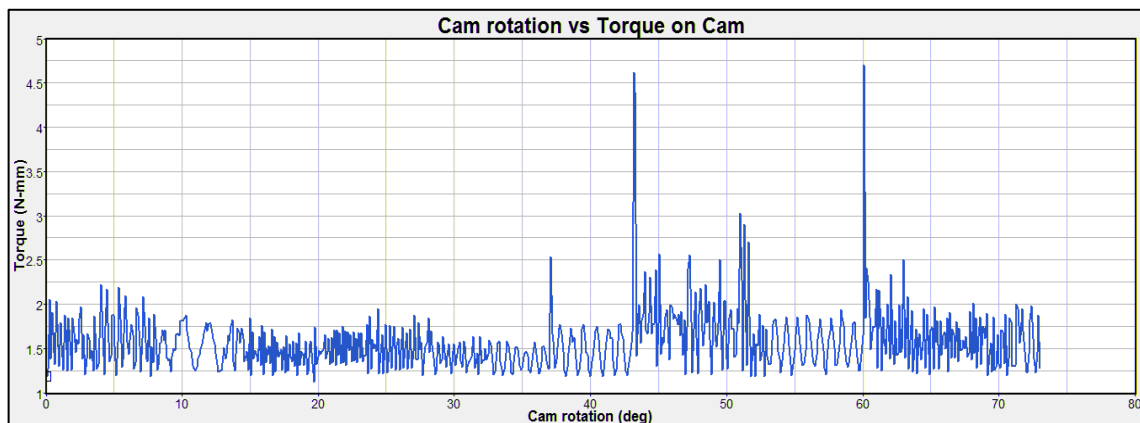


Figure 5.4: Cam rotation vs. Torque on cam at S=0.3, D=0.15

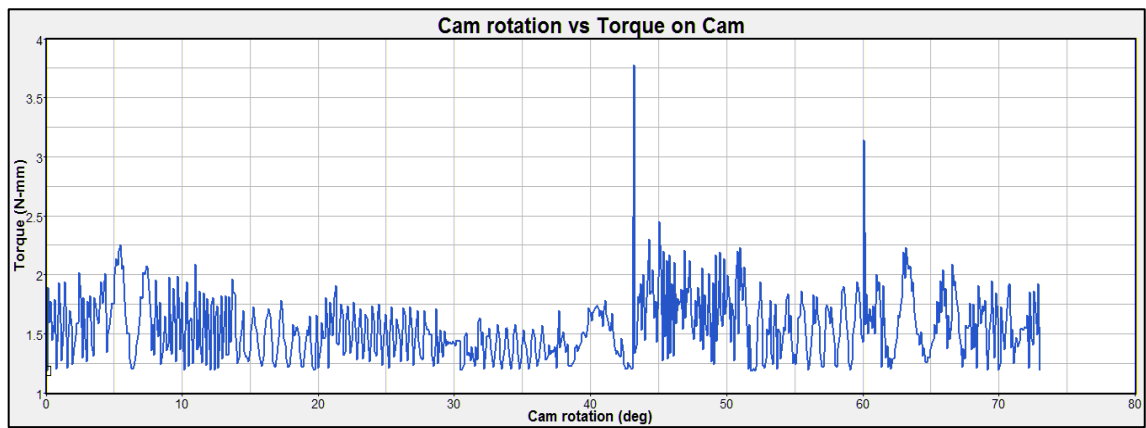


Figure 5.5: Cam rotation vs. Torque on cam at S=0.4, D=0.1

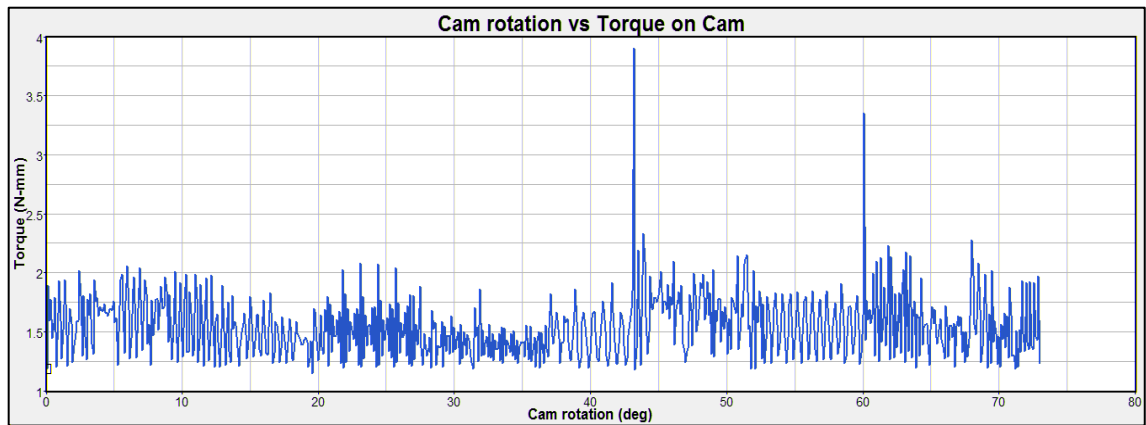


Figure 5.6: Cam rotation vs. Torque on cam at s=0.3, D=0.1

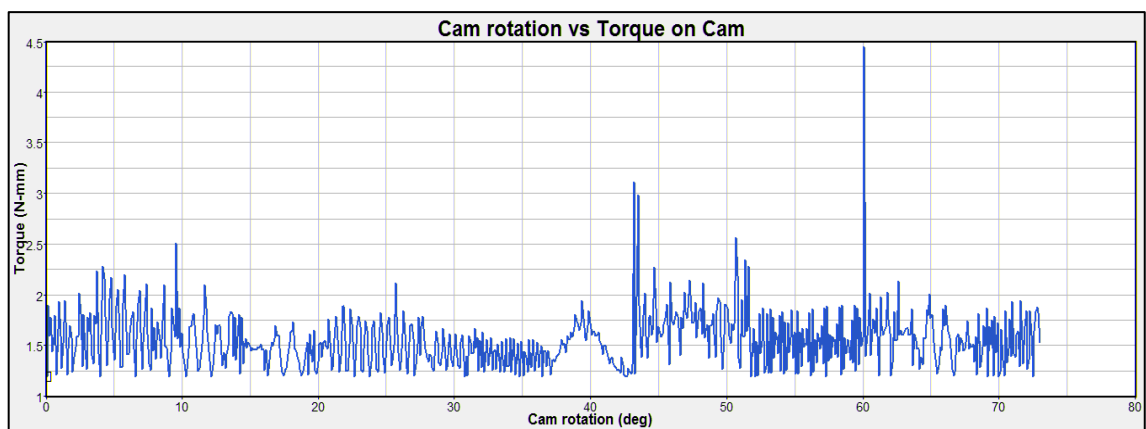


Figure 5.7: Cam rotation vs. Torque on cam at S=0.35, D=0.1

The results obtained for double link mechanism are shown in fig 5.8 to fig 5.12.

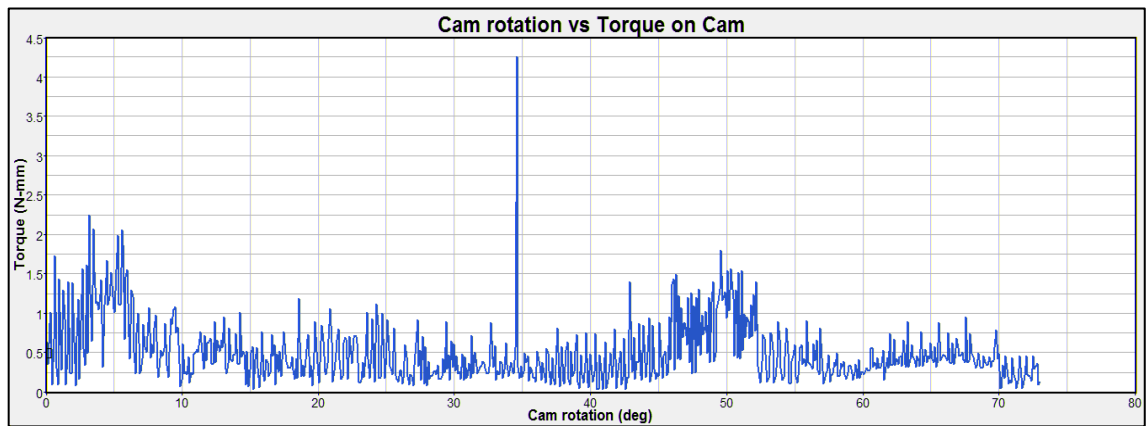


Figure 5.8: Cam rotation vs. Torque on cam at $S=0.25$, $D=0.1$

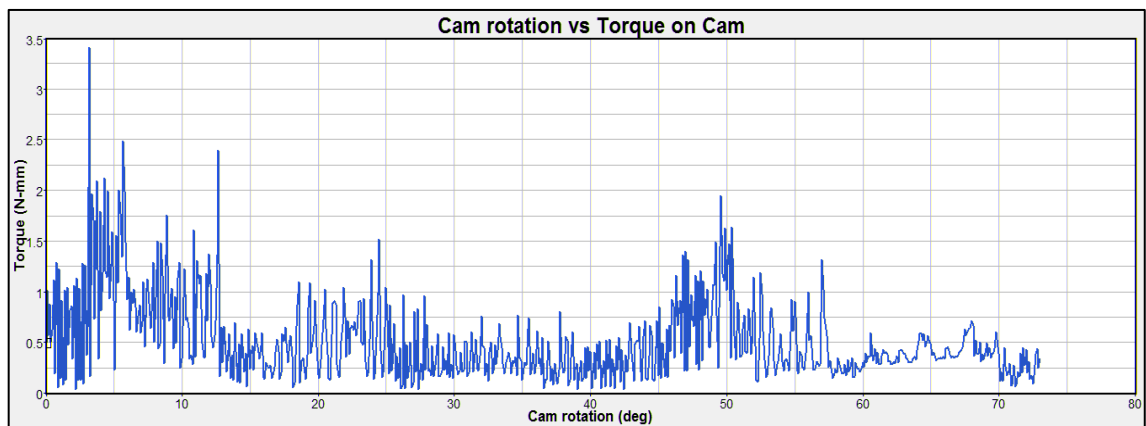


Figure 5.9: Cam rotation vs. Torque on cam at $S=0.3$, $D=0.15$

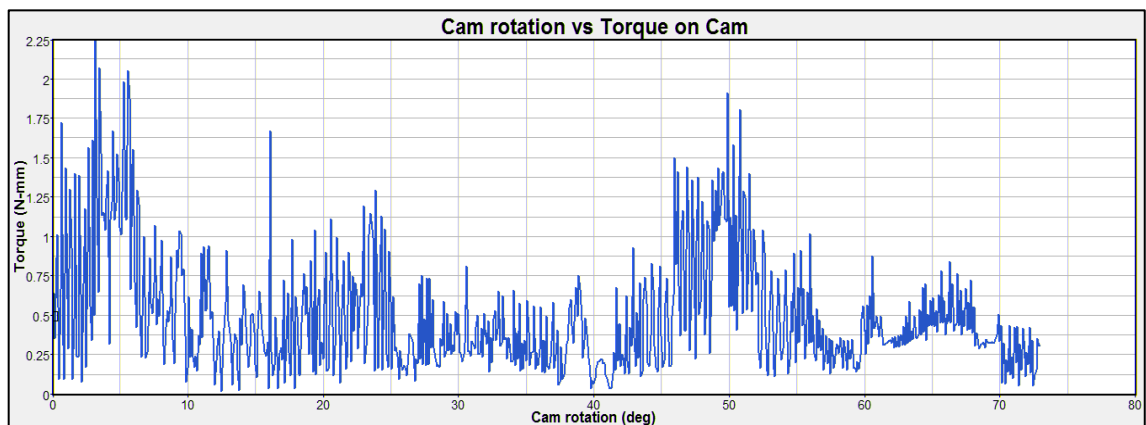


Figure 5.10: Cam rotation vs. Torque on cam at $S=0.4$, $D=0.1$

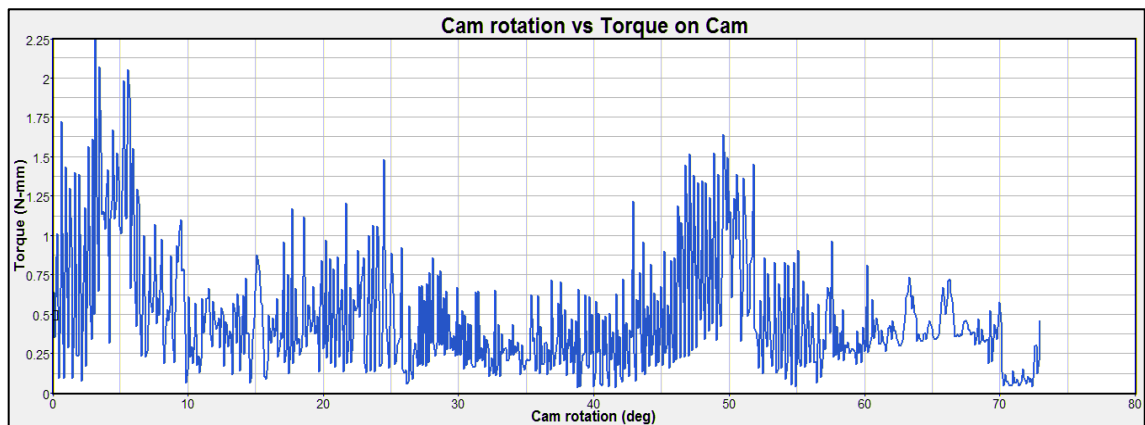


Figure 5.11: Cam rotation vs. Torque on cam at $s=0.3$, $D=0.1$

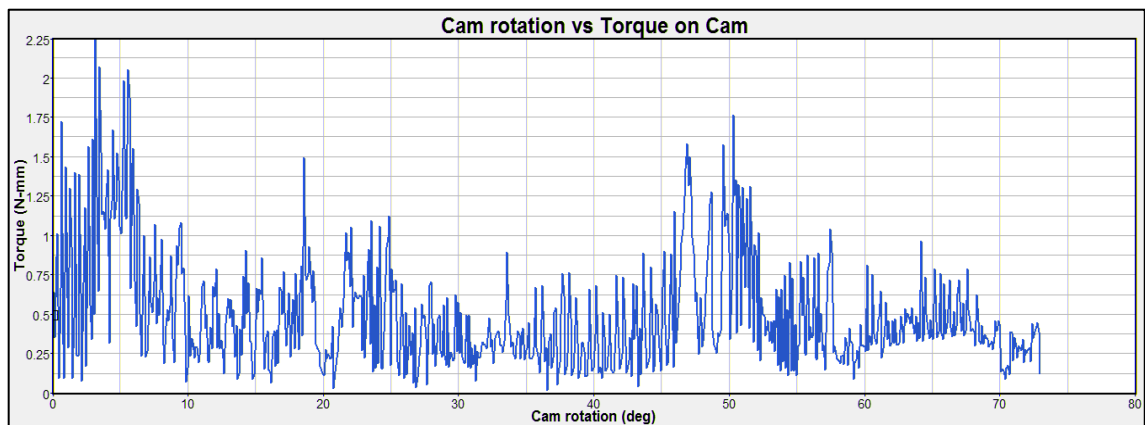


Figure 5.12: Cam rotation vs. Torque on cam at $S=0.35$, $D=0.1$

Without friction, the maximum torque obtained in single link mechanism is 2.8 N-mm. After friction value is incorporated, the maximum torque on cam obtained is 4.6 N-mm. Without friction, the maximum torque obtained in double link mechanism is 2.25 N-mm. but after friction value is incorporated, the maximum torque on cam obtained is 4.3 N-mm.

EFFECT OF FORCE DUE TO AIR PRESSURE ON DAMPER

6.1 INTRODUCTION

The air blown by the blower passes through the evaporator and/or the heater located inside the HVAC module and is thus cooled and/or heated up accordingly. There are openings provided in the cases for airflow in various modes. Five different modes are face, foot, bi-level (face/foot), defrost and foot/defrost. The HVAC module has a mechanism consisting of various links and a cam responsible for controlling the air flow going through these modes to the passenger cabin.

The face and foot damper are in contact with air. Due to the air pressure on the dampers, torque required to operate the cam will vary. The torque required to operate the cam should not be very high, as this would lead to passenger discomfort while using the various knobs on the control panel in the vehicle.

In this chapter, simulations are done by considering the air pressure on damper. Force is applied on the damper and the simulations are run. The result is obtained in the form of graph (cam rotation vs. torque required to operate the cam). The value of force (f) is varied and the result is analysed. In fig 6.1 to fig 6.4, force is applied at the point where the damper centre of gravity lies and in fig 6.5 to fig 6.7, force is applied at the centre of gravity of the damper and four other points on the damper face.

5.2 RESULTS

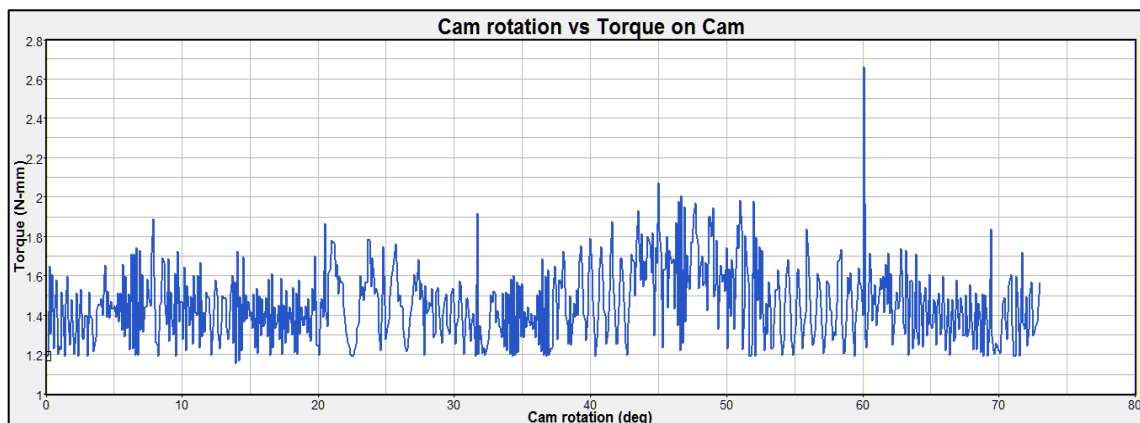


Figure 6.1: Cam rotation vs. Torque on cam at $f=0.5N$

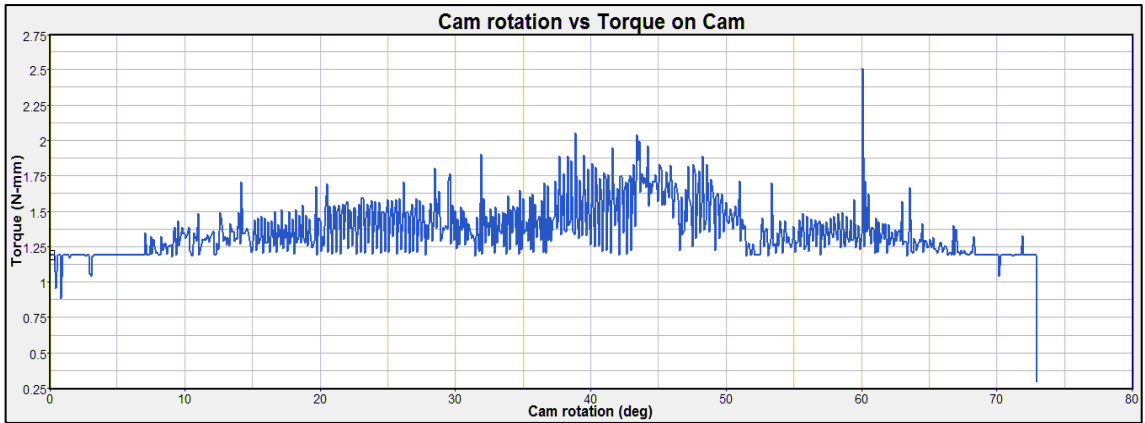


Figure 6.2: Cam rotation vs. Torque on cam at f=1N

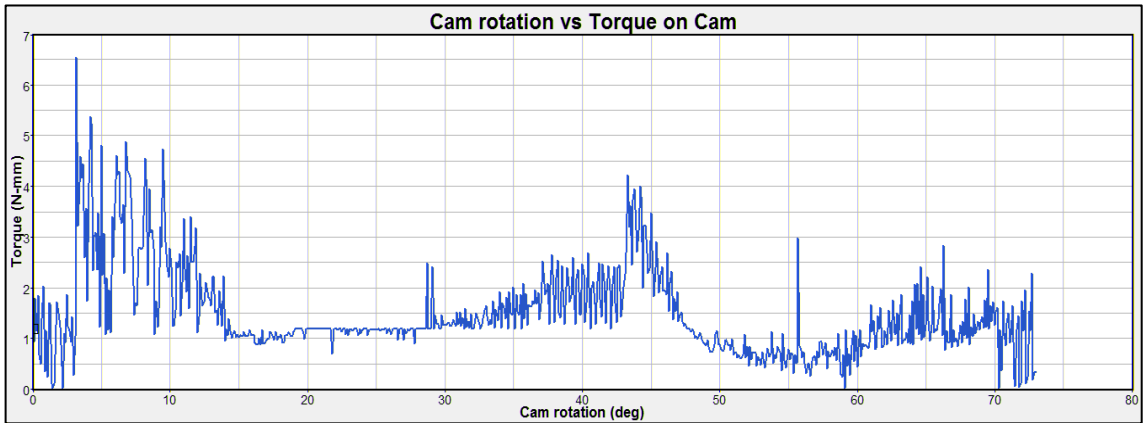


Figure 6.3: Cam rotation vs. Torque on cam at f=5N

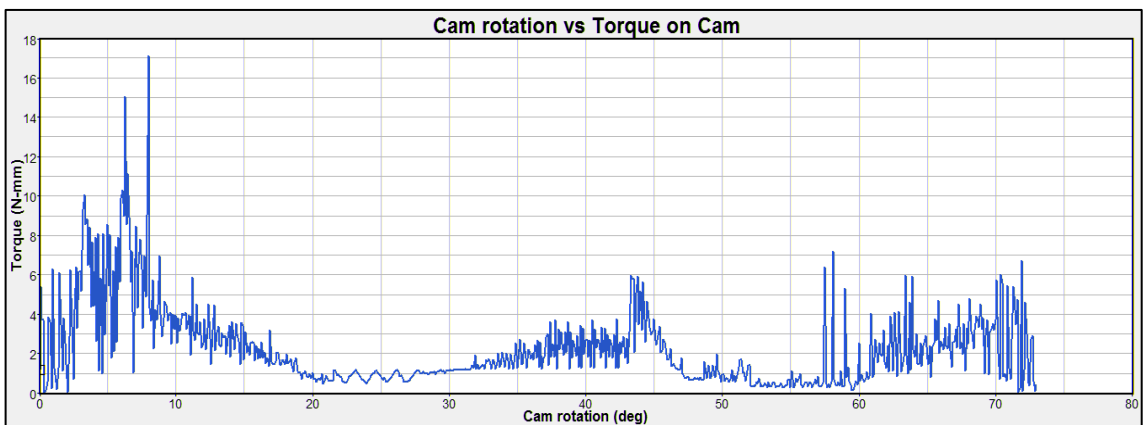


Figure 6.4: Cam rotation vs. Torque on cam at f=10N

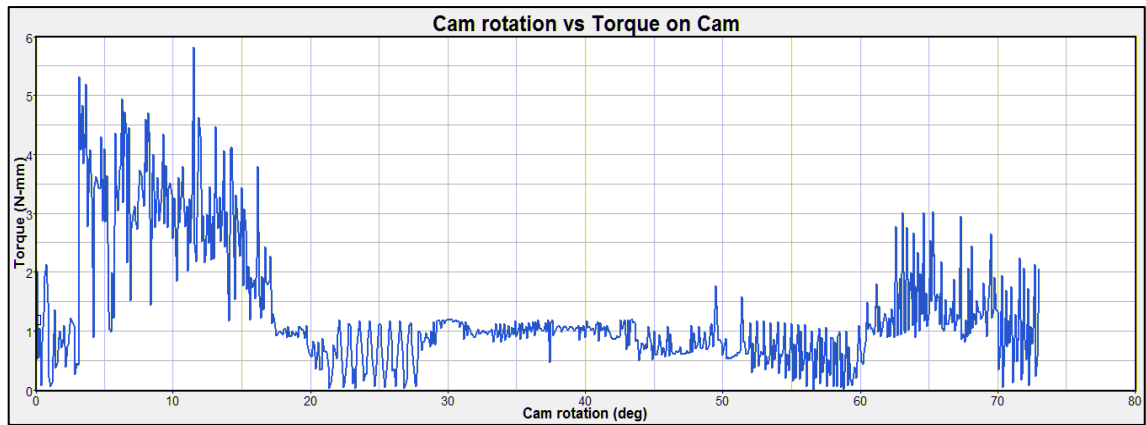


Figure 6.5: Cam rotation vs. Torque on cam at $f=1.25N$

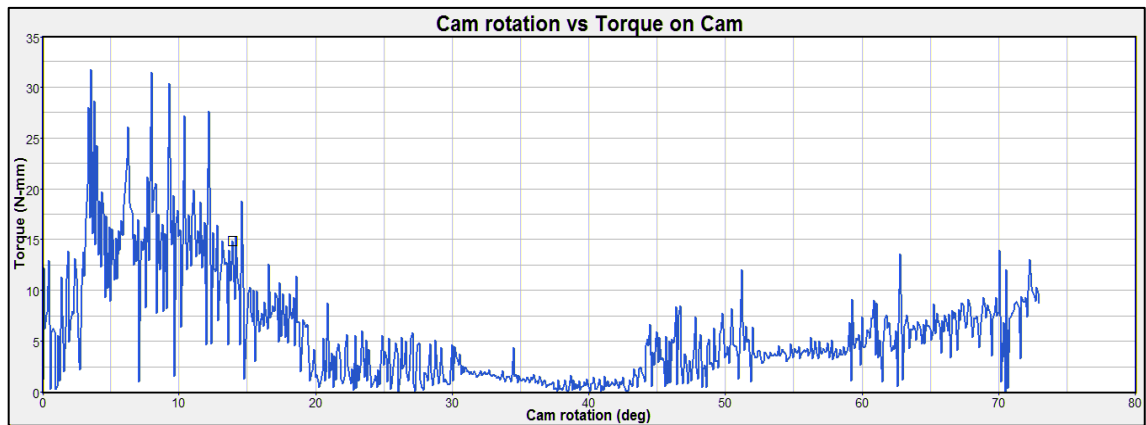


Figure 6.6: Cam rotation vs. Torque on cam at $f=10N$

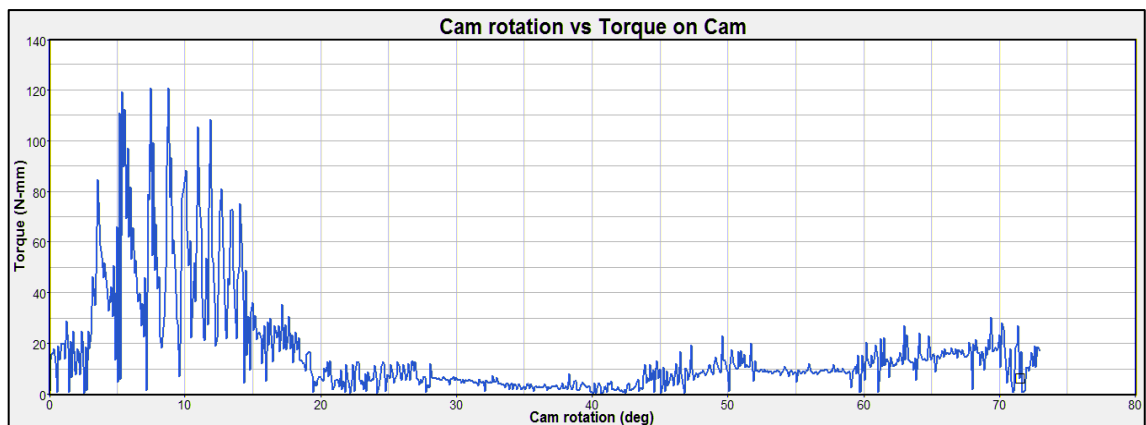


Figure 6.7: Cam rotation vs. Torque on cam at $f=20N$

These analyses are done by assuming the value of forces applied on the damper due to air pressure. If the exact value of force is known, it can be used in the proposed analysis procedure.

7.1 INTRODUCTION

Flexible multibody dynamics is the subject concerned with the computer modelling and analysis of constrained deformable bodies that undergo large displacements, including large rotations. The large displacement includes rigid body motion as well as elastic deformations. A flexible multibody system may consist of elastic and rigid components which are connected by joints and/or force elements such as springs, dampers, and actuators. Because of the joint constraints the displacements of the bodies in the system are not totally independent.

In this HVAC mechanism study, links are the critical part of the mechanism in which stress and strain produced w.r.t. time. So in this work, link is taken as a flexible body and other parts are rigid body. A tetra mesh is used for meshing this part. Element size used for meshing is 1 mm. The link is made of PVC (Plastic) material.

Properties of PVC material are:

Mass Density (ρ)	:	1.4e-006 kg/mm ³
Young's Modulus (E)	:	3 e+006 MN/mm ² (KPa)
Poisson's Ratio (ν)	:	0.4
Yield Strength	:	44500 MN/mm ² (KPa)

The above properties of PVC are assigned to the part.

A rigid element is a link from one node to another (or multiple nodes), where the motion of the nodes is governed by the degrees of freedom which we choose to connect. A rigid element is actually a constraint equation rather than an actual element. It can be used to give stiffness to the structure.

Two rigid elements (as shown in fig 7.1) are defined in the link at the centres of the holes so that stiffness is given at the nodes, on the surface of the holes. The nodes at the centre of holes are taken as independent nodes. The centre node connects with the nodes on the

surface of hole. Both centre points of the holes are taken as interface nodes. The part is converted into a flexible body and then the analysis is run.

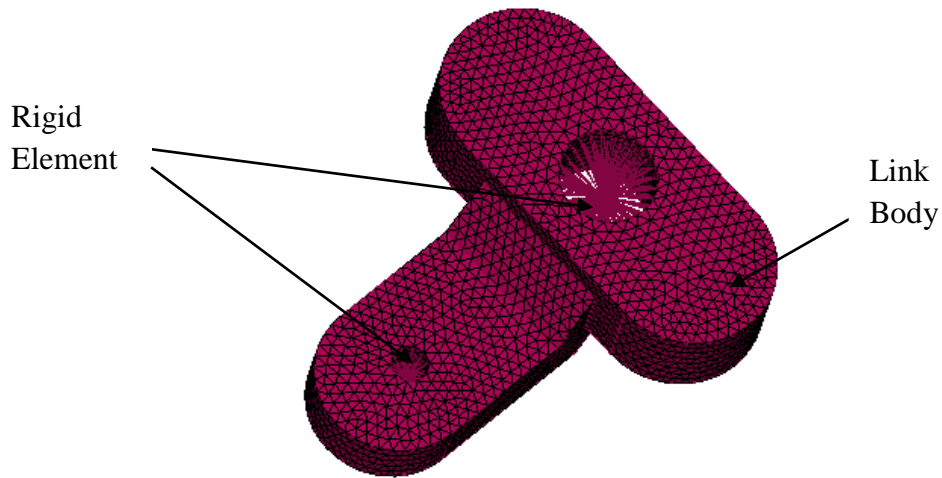
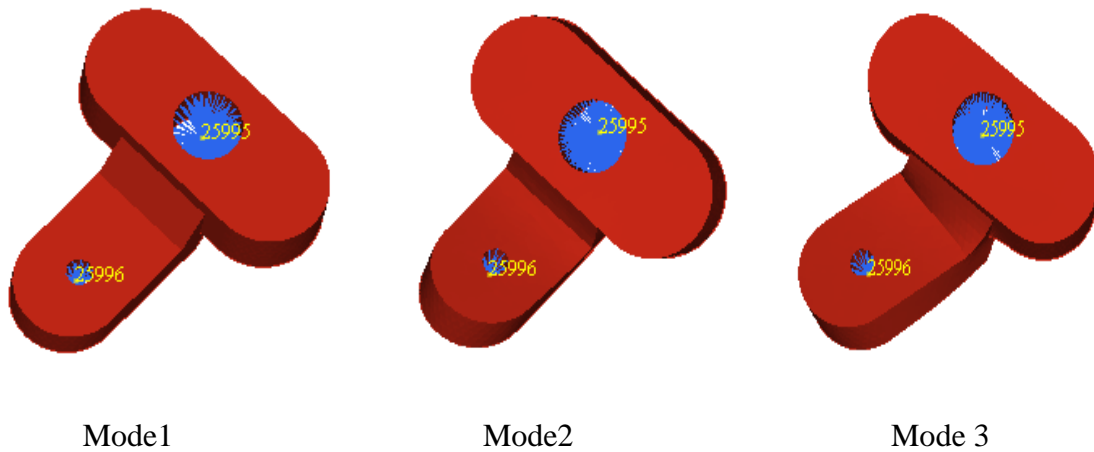
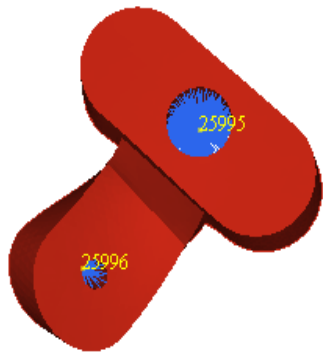


Fig 7.1 Link with mesh

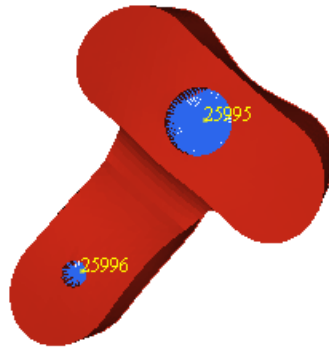
7.2 RESULTS

The results are obtained in the form of modal displacements of the link at different frequencies are shown below:

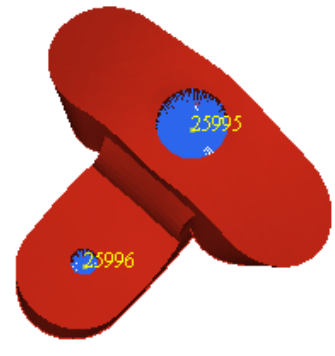




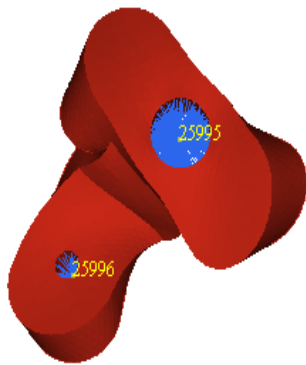
Mode 4



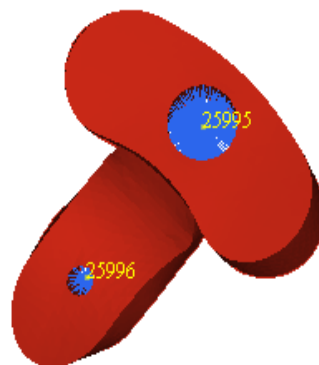
Mode 5



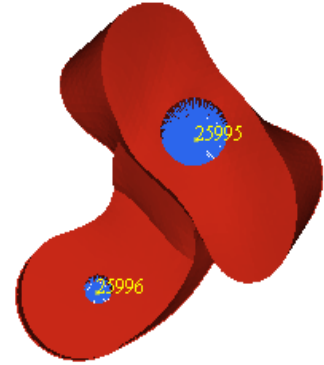
Mode 6



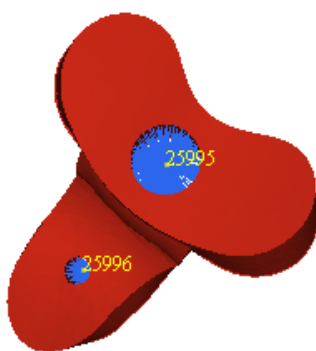
Mode 7



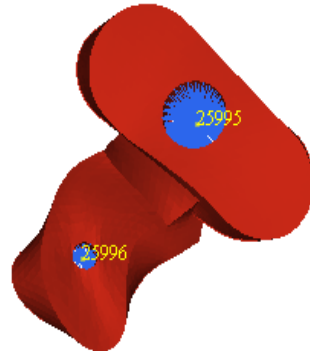
Mode 8



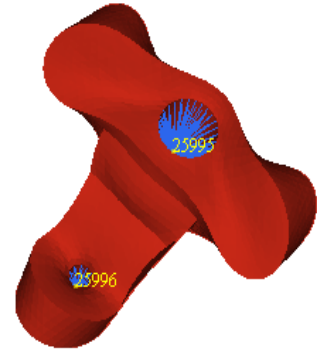
Mode 9



Mode 10



Mode 11



Mode 12

Fig 7.2 Modal shapes of link

7.3 FORCE ON LINK ANALYSIS

For stress analysis, first the force was analysed on the link body at different speeds. In kinematic analysis of HVAC mechanism, the output was defined the force on the link body. The analysis was run and the desired output was obtained. The output obtained in the form of a graph between cam rotation and torque on the link. So that maximum torque value was obtained during the full cycle of mechanism. Force value was calculated from the torque obtained. The analysis was run at different speeds to get the force output so that stress analysis could be done at that force.

The outputs obtained are shown below:

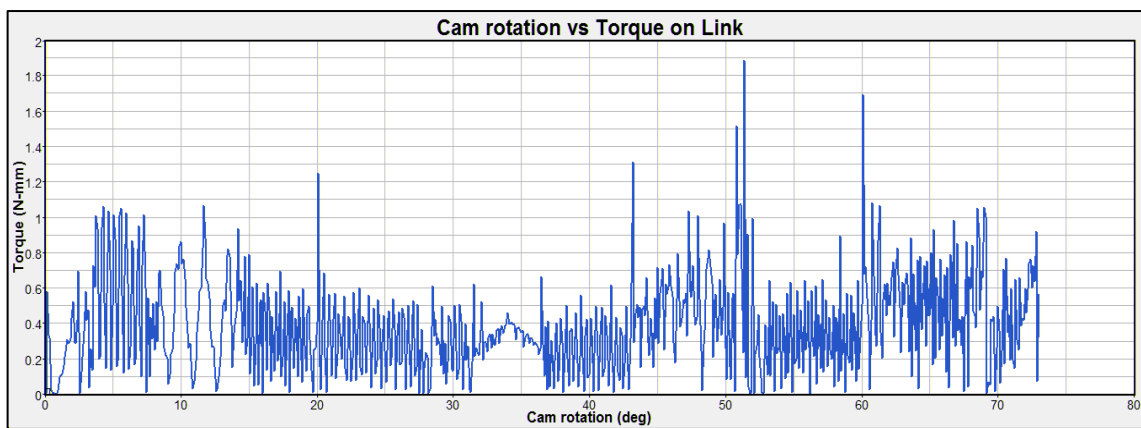


Figure 7.3: Cam rotation vs. Torque on Link at speed 10°/sec

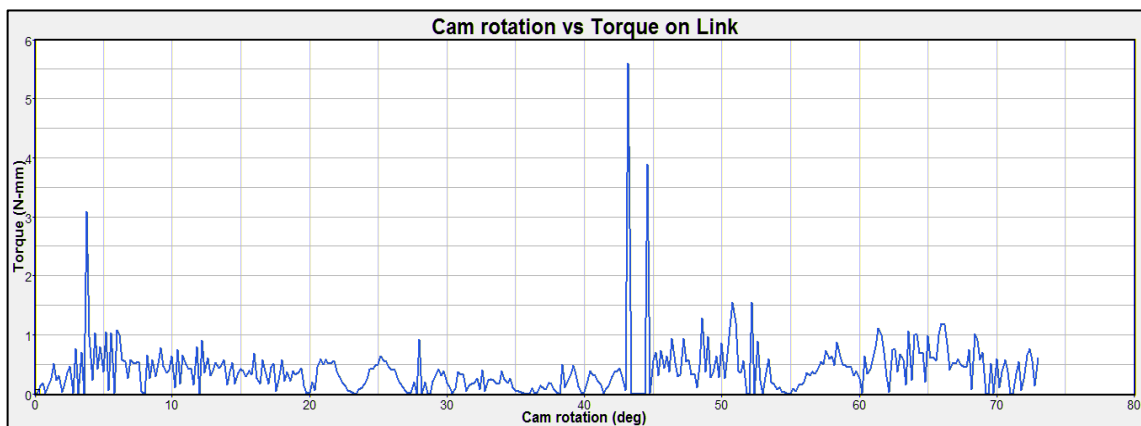


Figure 7.4: Cam rotation vs. Torque on Link at speed 20°/sec

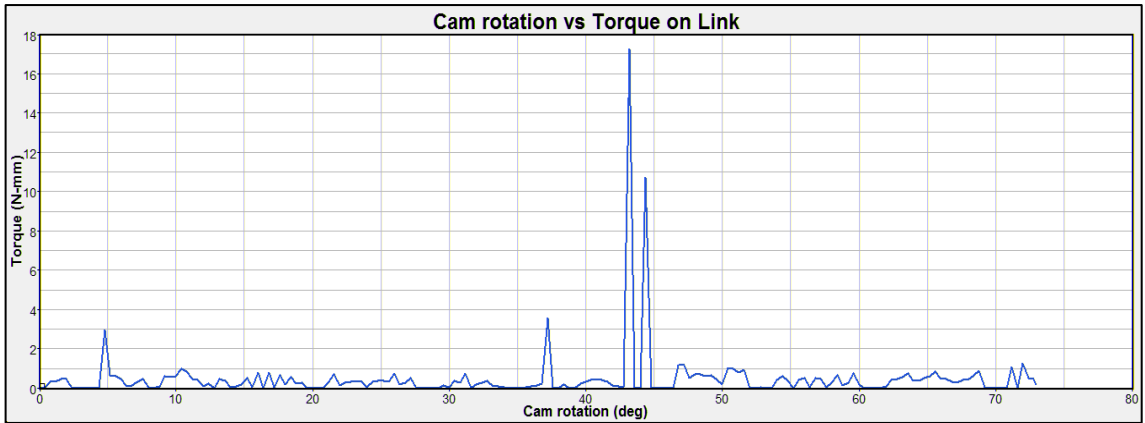


Figure 7.5: Cam rotation vs. Torque on Link at speed 40°/sec

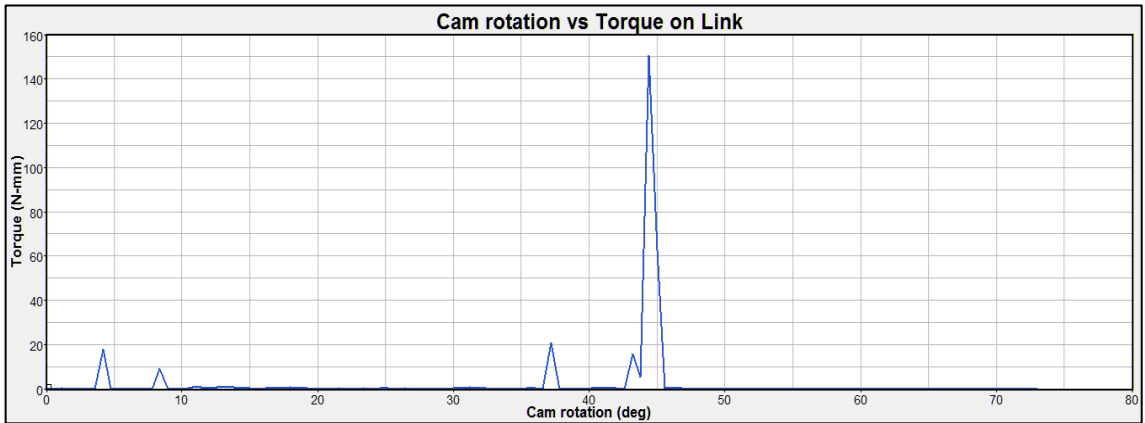


Figure 7.6: Cam rotation vs. Torque on Link at speed 60°/sec

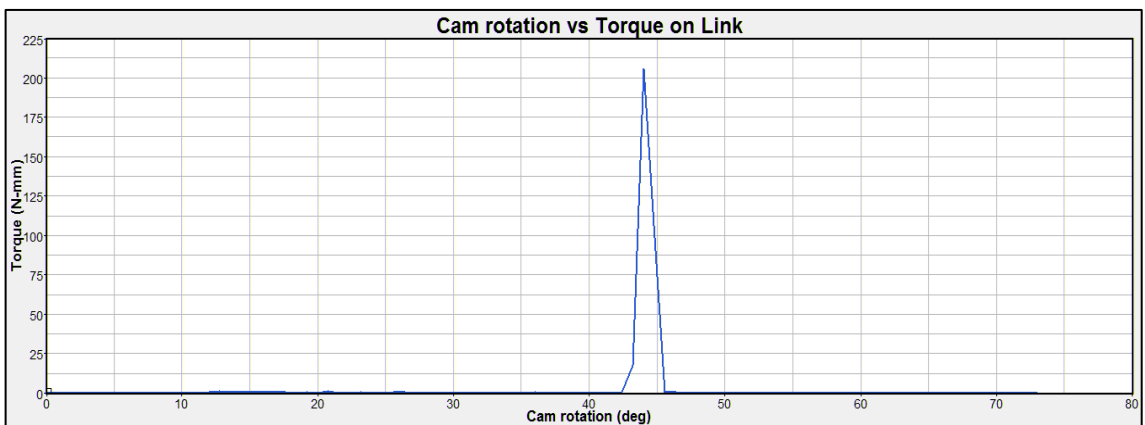


Figure 7.7: Cam rotation vs. Torque on Link at speed 80°/sec

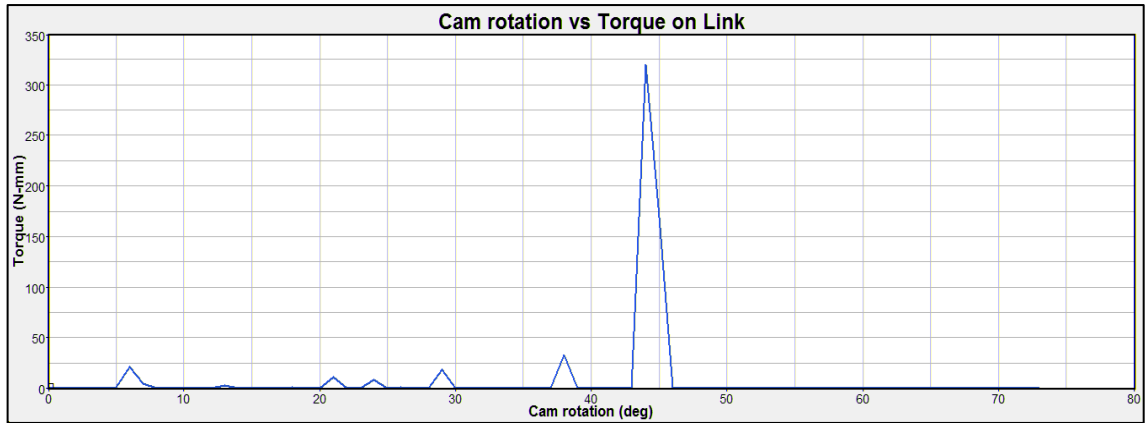


Figure 7.8: Cam rotation vs. Torque on Link at speed 100°/sec

With the help of the above graph, the value of force on the link was obtained which is given below:

Table 7.1 Force analysis

	1	2	3	4	5	6
Cam Speed (in °/sec)	10	20	40	60	80	100
Torque on link (in N-mm)	2	5.6	17	150	210	320
Force on Link (in N)	0.1	0.3	0.8	7.5	10.5	15

7.4 STATIC STRESS ANALYSIS

These values of forces are considered as the input for stress analysis of link. The force value was applied and the static analysis of link was run. The results are obtained from these analyses are given below:

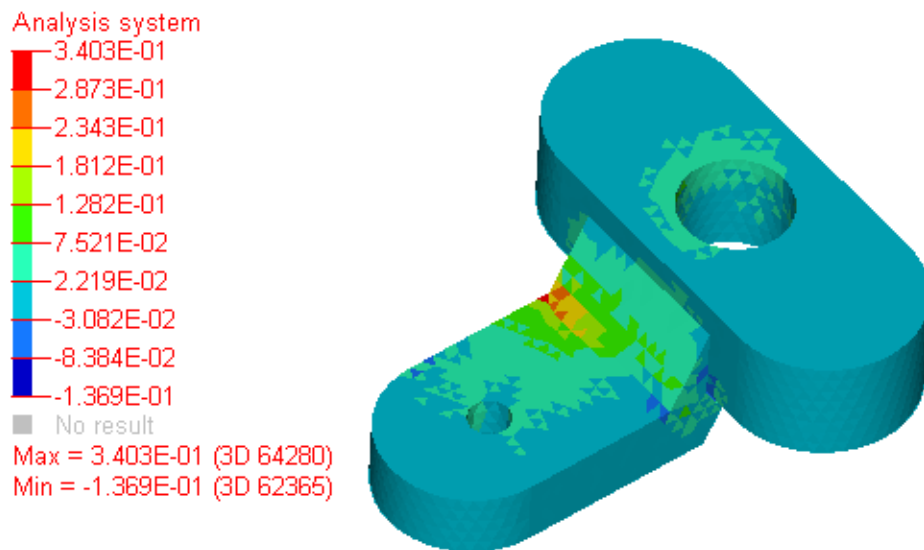


Fig 7.9 Stress analysis at speed of cam 10°/sec

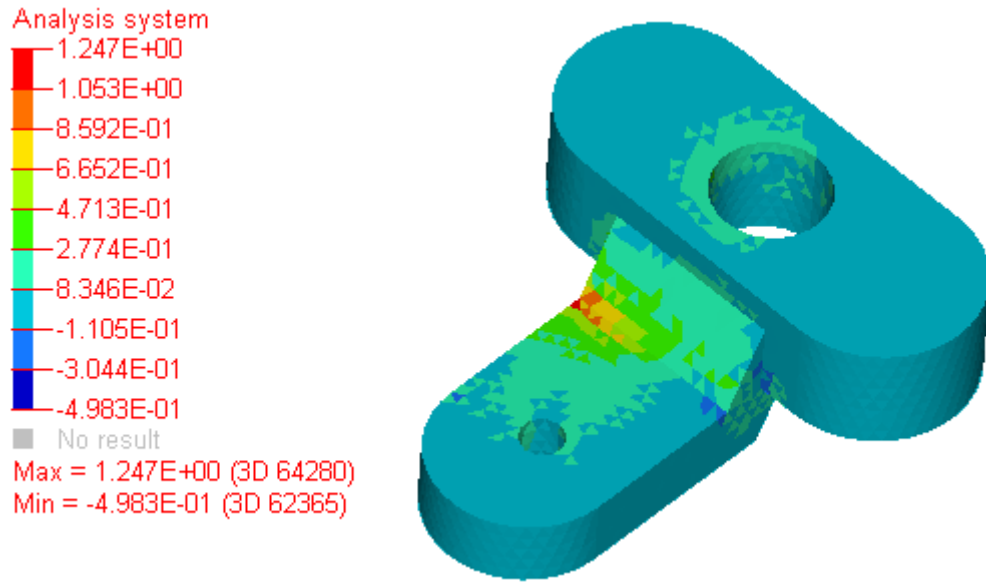


Fig 7.10 Stress analysis at speed of cam 20°/sec

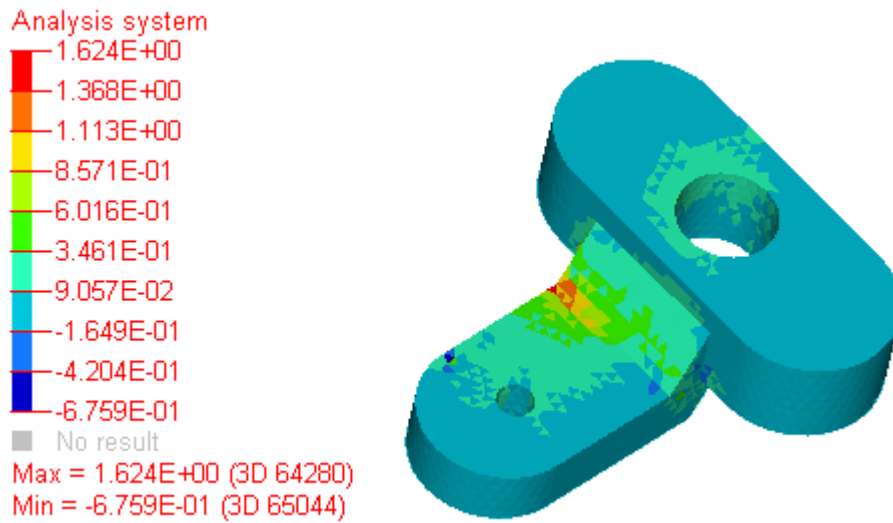


Fig 7.11 Stress analysis at speed of cam 40°/sec

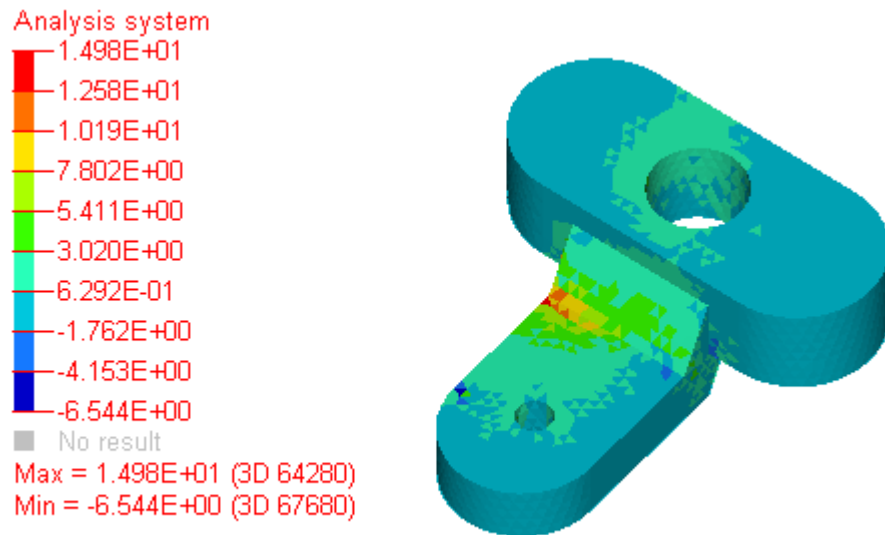


Fig 7.12 Stress analysis at speed of cam 60°/sec

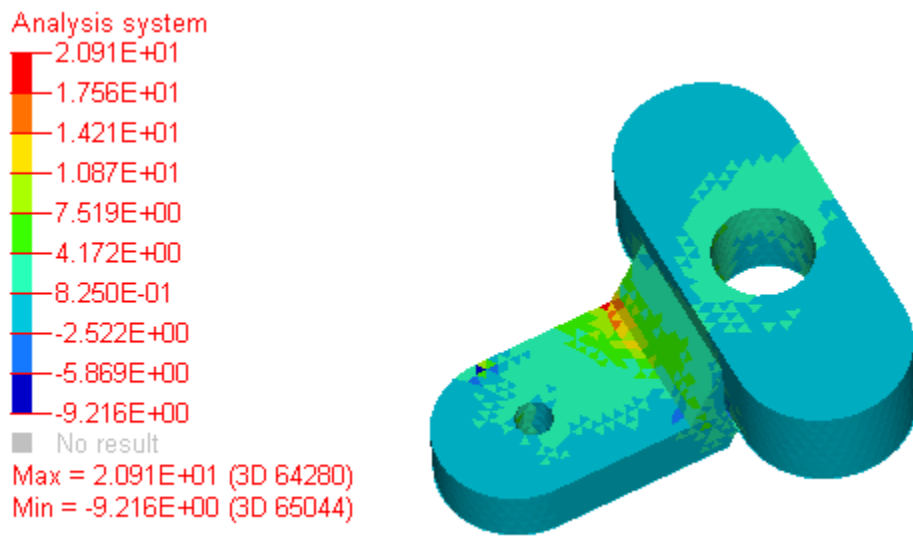


Fig 7.13 Stress analysis at speed of cam 80°/sec

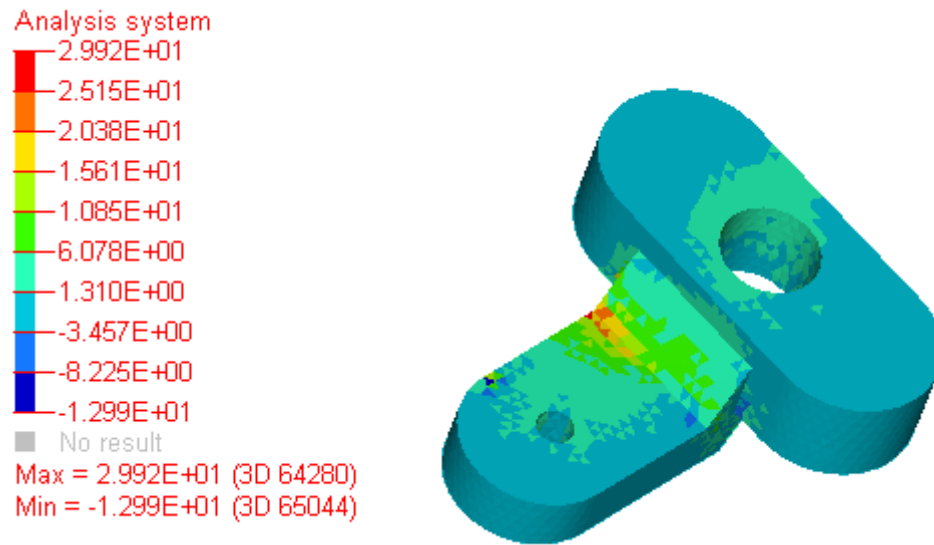


Fig 7.14 Stress analysis at speed of cam 100°/sec

CONCLUSION AND SCOPE FOR FUTURE WORK

8.1 CONCLUSION

An existing design of HVAC kinematic mechanism is studied and kinematically and dynamically analysed. The results obtained revealed the information about the relative motion and design of mechanism components. For the given problem two HVAC kinematic mechanisms are analysed, one with single link configuration and other with two link configuration. The assumptions include a constant angular velocity of the cam, and the rigidity of the parts in the mechanism. Using the same simulation methodology, kinematic analysis has been done for the two models and their results are compared. It is found that the torque required in the two link configuration is lesser than the one link design. Analyses are done by varying the speed of cam. It is found that the torque required to rotate the cam is increase by increasing the speed of cam. Analyses are done by considering the friction in between cam slots and pin. It is found that, without friction, the maximum torque obtained, in single link mechanism is 2.8 N-mm and obtained in double link mechanism is 2.25 N-mm. After friction value is incorporated, the maximum torque on cam is 4.6 N-mm and 4.3 N-mm. Analyses are also done by considering the air pressure on damper face. It is found that the torque required to rotate the cam is increased by increasing the air pressure on the damper face. Flexible body analyses are done and the stress at link is obtained. It is found that the stresses on the link are increasing by increasing the speed of cam.

With the use of the above approach, (1) a proper design of kinematics of linkages/damper movement can be arrived at with acceptable forces applied for various damper movements; (2) a significant cost saving, as the required number of physical prototypes is reduced.

Thus, the use of CAE tools leads to an easy visualization and comparison of data, thereby helping in the detection of problems early in the design cycle, reduced number of physical prototypes, resulting in significant saving of time and cost and last but not the least, more design iterations by incorporating simulation techniques.

8.2 SCOPE FOR FUTURE WORK

The present work can be further extended by incorporating the following:

- a) A cable (steel wire) connects the control knob on the dashboard of the car to the cam. When the knob is rotated, the wire pushes/pulls the cable pin present on the cam, thus rotating the cam clockwise/anticlockwise. The effect of this wire can be considered for further work.
- b) The design and analysis of the HVAC Kinematics parts can be automated using CAD and CAE tools. This can help in reduce the design cycle time, and ultimately the time-to-market for new models.
- c) The discussed methodology can be extended to the simulation of other automobile mechanisms like wiper mechanism etc.

REFERENCES

- [1] A. Srivastava, M. Gopikrishnan (2012), “Multi-Body simulation of Earthmoving Equipment using MotionView / MotionSolve”, *Proceeding of the HTC 2012, India*.
- [2] B. He, S. Wang, F. Gao, (2010), “Failure analysis of an automobile damper spring tower”, *Engineering Failure Analysis*, vol. 17, pp. 498–505.
- [3] B. Singh, D. Sing, J.S.Saini (2011) “The kinematic analysis of heating, ventilating and cooling module parts of automobile air conditioning system using CAE tools”.*M.E. Thesis, Thapar University, Patiala*.
- [4] C. Alexandru (2009) “Functional optimization of Windshield wiper mechanisms in MBS (multi-body system) concept”, *Bulletin of the Transilvania University of Brasov*, Vol. 2 (51) - 2009 • Series I.
- [5] F.J. Espadafor, J.B. Villanueva, M.T. Garcia, (2009), “Analysis of a diesel generator crankshaft failure”, *Engineering Failure Analysis*, vol. 16, pp. 2333–2341.
- [6] J.W. Yoon, Jung S.P., Park T.W., Park J.K. (2009) “Fatigue analysis of the main frame of overhead transportation vehicles using flexible multibody dynamics”, www.springerlink.com/content/1738-494x DOI 10.1007/s12206-010-0111-3.
- [7] M. Machado, P. Flores, D. Dopico, J. Cuadrado (2012) “Dynamic response of multibody systems with 3D contact-impact events: influence of the contact force model”, *EUROMECH Colloquium 524*.
- [8] M. Xingguo, Y. Xiaomei, W. Bangchun (2007), “Multi-body Dynamics Simulation on Flexible Crankshaft System”, *Proceeding of the 12th IFToMM World Congress, Besancon, France, June 18th-21th*.
- [9] N. Bertorelli, A. Gugliotta, R. Montanini, R. Vadori, (1998), “Structural crash analysis with ADAMS: a comparison between multibody and FEM approaches”, *Proceeding of the 12th European ADAMS Users’ Conference, Paris, Nov. 18th-19th*.
- [10] O.A. Bauchau, C. Ju, (2006), “Modeling friction phenomena in flexible multibody dynamics”, *Comput. Methods Appl. Mech. Engg.*, vol. 195, pp. 6909–6924.
- [11] P. Flores (2009), “Modeling and simulation of wear in revolute clearance Joints in multibody systems”, *Mechanism and Machine Theory*, vol. 44, pp. 1211–1222.
- [12] S. C. Jaiswal, Rahul Singh (2011) “Multibody dynamic analysis and simulation of engine model”, *International Journal of Engineering Science and Technology: 0975-5462* Vol. 3 No. 10 October 2011.

- [13] S. H. Lee, T.W. Park, J.K. Park, J.W. Yoon (2009) “A Fatigue Life Analysis of Wheels on Guide way Vehicle using Multibody Dynamics”, *International journal of precision engineering and manufacturing* Vol. 10, No. 5, pp. 79-84.
- [14] S. Magheri, M. Malvezzi, E. Meli, A. Rindi, (2011), “An innovative wheel–rail contact model for multibody applications”, *Wear*, vol.271, pp. 462-471.
- [15] S. Mukras, N.H. Kim, N.A. Mauntler, T.L. Schmitz, W.G. Sawyer, (2010), “Analysis of planar multibody systems with revolute joint wear”, *Wear*, vol. 268, pp. 643–652.